nature cities

Article

https://doi.org/10.1038/s44284-026-00501-4

Wildlife disease occurrence increases with changes to urban density, habitat connectivity and climate

Received: 17 October 2025

Accepted: 10 July 2026

Published online: 19 August 2026

Check for updates

Tiziana A. Gelmi-Candusso[1] ✉, Maureen H. Murray[1] ✉, Peter Rodriguez[2], Julia Angstmann[3], Summer Fink[4], Marie-Josee Fortin[2], Travis Gallo[5], Patrick Gentry[6], Daniela Guerrero[4], Jeffrey D. Haight[7], Sophia Hara[8], Mark Jordan[9], Michel T. Kohl[4], Jesse S. Lewis[7], Robert Long[10], Péter K. Molnár[2,11], Maia Mortimer[11], Brent R. Patterson[12], Sage Raymond[13], Katie Remine[10], Travis Ryan[3], Carmen Salsbury[3], Christopher J. Schell[14], Catherine Shier[15], Colleen C. St. Clair[13], Cassondra J. Stevenson[13], Juan S. Vargas Soto[11], Lisa Wayne[16], Tyler Wheeldon[12], Seth Magle[1] & Mason Fidino[1]

Increasing wildlife disease has been identified in urban areas, but the drivers of this increase remain unknown. Here, leveraging multi-city biomonitoring efforts across North America, we assessed whether greater occurrence of disease was correlated with urban characteristics, habitat connectivity loss and climate change. We focused on sarcoptic mange (*Sarcoptes scabiei*), an emerging panzootic disease, in coyotes (*Canis latrans*) using camera-trap images. Locally, disease occurrence was greater at sites with a higher urban intensity and in proximity to connectivity corridors. At the continental scale, disease occurrence was greater in cities with a higher human population density and fewer connectivity corridors. Following projected urban growth and climate change, we forecast an increase in mange occurrence across cities by 2050, most prominently at northern latitudes driven by a combined effect of urban densification and milder winters affecting host space-use overlap and host and mite survival. Urban planning for greater habitat connectivity and proactive disease management policies can improve wildlife welfare and limit the economic effects of zoonoses.

Global changes in urbanization, habitat fragmentation and climate affect wildlife disease dynamics[1,2], with cascading effects for public health, wildlife health and conservation. These global changes are interconnected but rarely studied together[3], which hinders our ability to anticipate their combined impacts on disease transmission. Local empirical studies and global syntheses of wildlife disease dynamics are common[4,5], but few studies bridge the gap to quantify the relative contribution of local processes and broader regional phenomena. Hence, regional variation, in urban density, landscape configuration and climate, limits our ability to extrapolate research results beyond single-city studies. In addition, differences in how urbanization is described and in data collection methods across empirical studies limit generalizable inferences and predictions about wildlife disease dynamics[6].

Large-scale standardized data collection efforts can help address this critical step to understand and predict how global change shapes wildlife disease dynamics. Emerging large-scale biodiversity monitoring networks, such as the Urban Wildlife Information Network (UWIN)[7], provide an opportunity to address the gap between local

A full list of affiliations appears at the end of the paper. ✉e-mail: tgelmicandusso@lpzoo.org; maureenmurray@lpzoo.org

empirical studies and global syntheses by generating consistent, systematic and regularly harmonized spatiotemporal data on wildlife at a continental scale. In UWIN partner cities, camera traps deployed in a standardized design along an urban gradient facilitate large-scale research on diseases with visible signs that can be detected through passive observation[8].

One widespread wildlife disease with signs of infection visible on camera trap images is sarcoptic mange, a highly contagious disease caused by the mite *Sarcoptes scabiei*. Sarcoptic mange affects at least 148 mammalian species, including humans, domestic animals and wildlife[9]. The host range for sarcoptic mange continues to expand, with nine new host species being infected per decade since 1970, leading to its consideration as an emerging panzootic disease at the human–livestock–wildlife intersection[9]. Sarcoptic mange impairs host immune response, thermoregulation and key behaviors such as feeding and resting, thereby reducing fitness and increasing the risk of secondary infections that can lead to host mortality[10,11]. In some cases, uncontrolled disease spread has led to mass mortality events[11] and population declines in endangered species[12]. Shifts in behavior and body condition may lead to infected animals being more reliant on human-associated foods[13,14], which can lead to increased human–wildlife conflict[15]. Additional human–wildlife conflict can be caused by spillover to humans, causing a mild form of scabies[16], and to domestic animals, causing urticarial lesions and secondary bacterial and fungal infections requiring veterinary treatment and having a financial impact for owners[17]. Therefore, sarcoptic mange is a growing One Health issue[18] at the intersection of wildlife, human and domestic animal health that causes biodiversity loss and has economic costs and public health impacts.

Sarcoptic mange mites are transmitted to susceptible hosts directly through contact with infected mammals or indirectly by encountering mites in shared environments[19]. This transmission mode is shared across other wildlife diseases relying on invertebrates, such as vector-transmitted diseases and most parasites, making sarcoptic mange a model for informing the status and spread of other wildlife diseases. For diseases relying on direct and indirect host contact, factors that affect host space use and encounter rates with invertebrates, such as land-use change via urbanization, can influence disease transmission dynamics[20] (Fig. 1).

Urbanization has been associated with increased sarcoptic mange occurrence and mortality, especially in carnivores, for example, raccoon dogs (*Nyctereutes procyonoides*)[21], San Joaquin kit foxes (*Vulpes macrotis mutica*)[22], red foxes (*Vulpes vulpes*)[23,24] and coyotes (*Canis latrans*)[8,25]. Carnivores living in urban environments may be more susceptible to mange infection due to changes in diet quality or exposure to contaminants[15,26,27]. Carnivores may also experience higher rates of parasite transmission if the availability and configuration of green spaces promotes shared space use among diseased and susceptible individuals[14,28–30]. For example, urbanization can concentrate hosts along movement corridors and remnant habitat, potentially increasing encounter rates with mites in contaminated environments[30], as suggested by higher blacklegged tick densities (Lyme disease risk) found along movement corridors[31]. Potential changes in encounter rates and spatial overlap among hosts highlight how urban planning and the resulting changes in habitat configuration in urban areas can elevate wildlife disease risk.

Variation in climate also shapes wildlife disease dynamics by impacting host survival and off-host pathogen survival. Hosts infected with mange are more likely to die in colder temperatures owing to hair loss and thermal stress[32]. As such, infected animals can survive longer in warmer climates, providing more opportunities for parasite transmission. For parasites such as *S. scabiei* mites, off-host survival depends strongly on temperature and humidity[33,34]. Therefore, any impacts of urbanization on mange may be mediated by the influence of climate on host physiology and mite survival[35] (Fig. 1). As urbanization and climate change accelerate[36,37], we expect urban wildlife disease dynamics to shift. Hence, integrating urban growth and climatic projections into disease models will be key to forecast continental-scale shifts in wildlife disease occurrence.

Here, we analyzed standardized camera trap data from ten North American cities to evaluate whether wildlife disease occurrence is associated with urbanization, habitat connectivity and climate using sarcoptic mange as a model. Building on prior work[33], we extended a multistate autologistic occupancy model to account for within- and among-city environmental factors and temporal processes such as climate and urban growth. This multi-city analytical framework allows us to explore local patterns in the distribution of diseased hosts in urban areas and geographical patterns in the intensity of mange occurrence across the North American continent, hence quantifying the relative contribution of both local and regional processes on disease occurrence, something rarely possible in wildlife disease research. We hypothesized that at the continental scale, cities would have a higher occurrence of diseased hosts (that is, at more sites) if they had warmer, more humid climates favoring host and mite survival and if the city's habitat availability and configuration promoted space-use overlap among hosts. We also hypothesized that, at sites within cities, the occurrence of diseased hosts would be higher where hosts were more likely to share space, specifically areas key for habitat connectivity within more urbanized areas (for example, movement corridors; Fig. 1). To understand how disease risk will change over time, as urbanization intensifies and climate changes, we also forecasted mange occurrence in these ten cities by 2050 under the least and most sustainable future Shared Socioeconomic Pathways (SSP126 and SSP585)[38]. By quantifying how wildlife disease dynamics are shaped spatiotemporally by local and regional processes, this work helps to build a framework to better understand and forecast wildlife diseases in our rapidly changing world.

Results

We deployed 487 total cameras in ten cities, with 25–112 cameras in each city ($\bar{x} = 48.6 \pm 0.8.4$). The sampling effort was between 367 and 4,568 camera weeks per city ($\bar{x} = 1,604.0 \pm 417.3$), for a total effort of 16,040 camera weeks for the entire study. We observed coyotes in all cities and at 78% of sites across all cities (355 of 487 sites, minimum (min) of 36%, maximum (max) of 100% of sites per city); totaling 8,485 coyote images (min of 237 and max of 2,811 images per city). From all coyote images collected, 1,046 images (12.3%) had a coyote with visible mange signs (min per city, 10 out of 856, 1.2%; max, 576 out of 2,811, 20.5%). Mange was present in all cities, on average at 40.5% of sites in each city (min of 8.7% and max of 75%; Extended Data Table 1). Based on our model, average coyote occupancy across cities was 0.82 (90% Bayesian credible intervals (BCI), 0.48 to 0.96) and, at sites where coyotes were present, there was an average 0.50 (90% BCI, 0.31 to 0.76) probability of a coyote having signs consistent with sarcoptic mange (hereafter, mange occurrence; Extended Data Fig. 1).

We found opposing effects of urbanization on coyote and mange occurrence. To represent urbanization degree, we used the first principal component of a principal component analysis (PCA, proportion of variance explained of 0.78), which increased in value with increasing building density (+0.62) and human population density (+0.56) and decreasing natural vegetation cover (−0.66). Overall across cities, we found strong evidence (that is, 0.95 probability of the posterior effect having the identified direction) of coyote occupancy decreasing with local levels of urbanization ($\beta^{\psi}_{\mathrm{URB}} = -0.32$; 90% BCI, −0.66 to 0.02), and moderate evidence (that is, 0.79 probability of effect direction) of mange occurrence being higher for coyotes in sites with higher levels of urbanization ($\beta^{\omega}_{\mathrm{URB}} = 0.26$; 90% BCI, −0.28 to 0.86; Fig. 2a and Extended Data Table 2). These results suggest that as urbanization doubles, the probability of coyote occupancy decreases by 21%, while the probability of mange occurrence may increase by 17%. However, the intensity in the association between urbanization and mange

https://doi.org/10.1038/s44284-026-00501-4

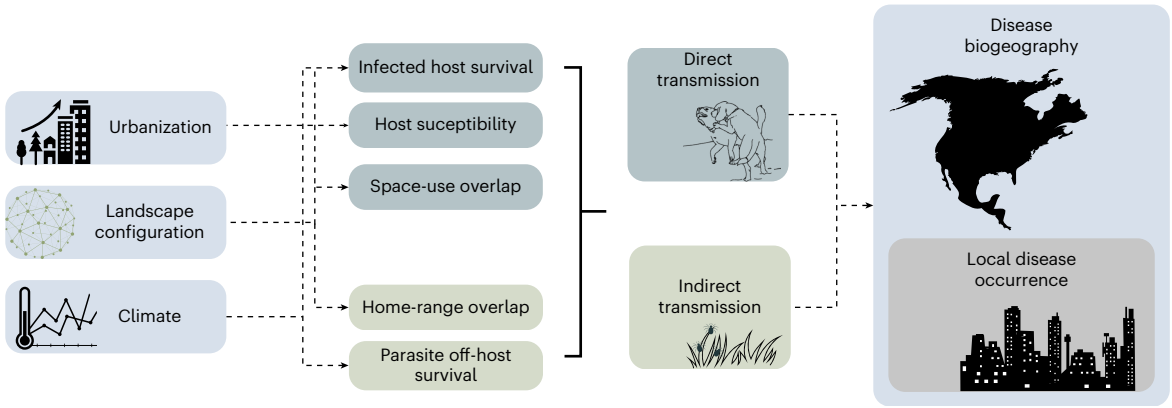

Fig. 1 | Factors impacting transmission dynamics following changes in urbanization, habitat connectivity and climate. Urbanization intensity, landscape configuration and climate define host survival, susceptibility and their space-use and home-range overlap, while climate impacts host survival and parasite off-host survival. These factors influence direct and indirect transmission rates, potentially leading to differences in disease occurrence at a local scale (within cities) and at the continental scale (among cities) and hence the local and global disease distribution.

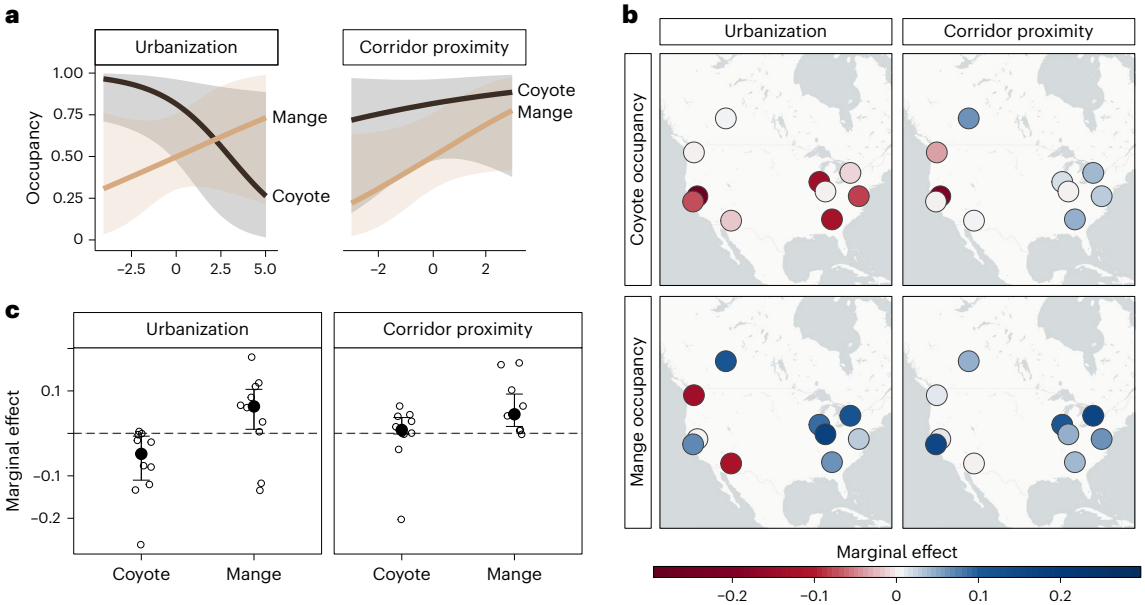

Fig. 2 | Coyote and mange occurrence differences at the local scale following urbanization intensity and proximity to movement corridors. a, Predicted coyote and mange occupancy as site-level urbanization and connectivity values increase. The line denotes the median predicted occupancy, and shaded areas denote 95% credible intervals. **b**,**c**, Marginal effect of site-level urbanization and proximity to corridors on average coyote and mange occupancy across cities ($n = 10$); median of marginal effect across cities (black point) and the difference between top and bottom quartiles of the marginal effect across cities (whiskers) (**b**) and geographical distribution of median marginal effects (**c**). Map tiles in **b** from CartoDB and map data © OpenStreetMap contributors.

occurrence varied across cities (Fig. 2b,c and Extended Data Table 2). Cities with a weaker association between mange occurrence and urbanization were surrounded by abundant natural habitat, mainly forest surface cover—except for Phoenix, which is surrounded by the Sonoran Desert—prime habitat for coyotes. Cities with a stronger association between mange occurrence and urbanization were surrounded predominantly by agricultural areas (33–49% agricultural surface cover versus 0.1–4% agricultural surface cover in cities with weaker associations) and lower natural cover (15–33% natural surface cover versus 50–89% natural surface cover); these were Chicago, Toronto, Edmonton and Indianapolis (Extended Data Fig. 2). Overall, sites with a higher population and building density and lower availability of green areas were less likely to be used by coyotes, but those coyotes had a higher likelihood of showing signs of mange, especially when habitat availability outside the city was limited.

Similarly, we found a relationship between coyote and mange occurrence and the position of a site relative to the habitat connectivity network, that is, areas that have a high potential to act as movement pathways for coyotes. We identified such movement pathways with Omniscape[39,40], whereby outputs are provided in units of cumulative current density, indicating how frequently a map unit occurs in predicted movement paths between other map units[41]. We confirmed the relationship between higher current density map units and more frequent coyote movement using Global Positioning System (GPS)-collared coyote data from two cities (Supplementary Section 1). The position of each site relative to the habitat connectivity network was defined through the first principal component of a PCA (proportion of variance explained, 0.65), increasing with vicinity to a movement corridor (+0.71, identified as the top 10% of a study area's current density values[42]) and increasing the surrounding mean current density value (+0.71, 1-km buffer). For simplicity, we called this variable 'proximity to corridor'. We found coyote occupancy had moderate evidence of being positively associated with proximity to corridor (0.69 probability of effect direction; $\beta^{\psi}_{\mathrm{CONN}} = 0.10$; 90% BCI = −0.32, 0.59). By contrast,

https://doi.org/10.1038/s44284-026-00501-4

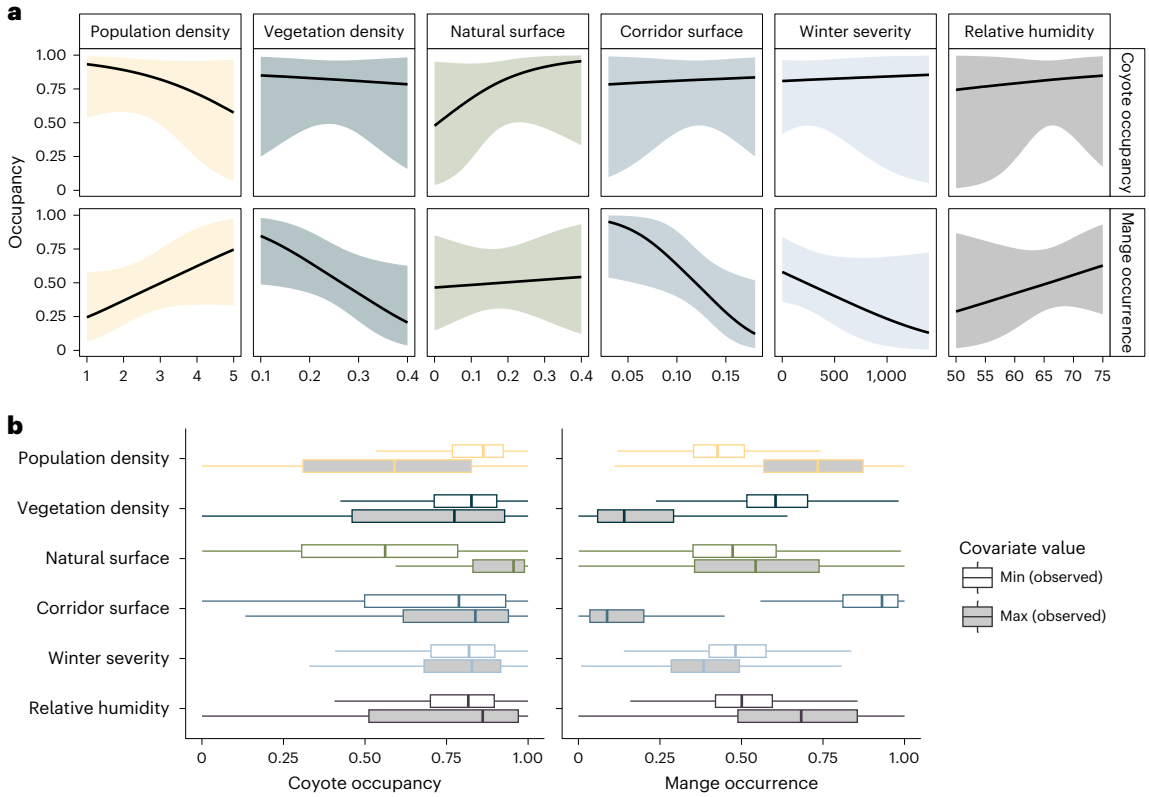

Fig. 3 | Factors influencing coyote and disease occurrence at the continental scale. a, Predicted occupancy changes in coyote (top) and coyotes with mange symptoms (bottom) across city-level environmental factors including, from left to right, urban human population density; urban vegetation density index, habitat availability in terms of total surface area occupied in a city by natural areas; availability of movement corridors, in terms of total surface area of a city classified as the top 10% of current density values within the study area; winter severity following chilling-degree days; and annual mean relative humidity. The line denotes the median predicted occupancy, and shaded areas denote 90% credible intervals given the posterior effects of 300,000 iterations. **b**, Distribution of predicted mange occurrence across model iterations (*x* axis) following the expected change in occurrence across covariates (*y* axis), comparing mange occurrence predictions between the minimum covariate value observed in our study (white) against the maximum covariate value observed (gray). The box plot illustrates the variations in mange occurrence across iterations, highlighting the median predicted occurrence (center), top and bottom quartiles (bounds of box) and extending between the minimum and maximum values across iterations (whiskers).

we found strong evidence (0.93 probability of effect direction) that mange occurrence was positively associated with proximity to corridor ($\beta^{\omega}_{\mathrm{CONN}} = 0.53$; 90% BCI, −0.05 to 1.19; Fig. 2a and Extended Data Table 2). These results suggest that a site closer to a movement pathway may have on average 4% higher coyote occupancy than a site twice as far from a movement pathway; while it will have an average of 33% higher likelihood of mange occurrence. The association between mange occurrence and proximity to corridor was consistent across cities, with a positive marginal effect in nine out of ten cities (Fig. 2b,c and Extended Data Table 2). However, the degree of association varied, whereby cities with a lower availability of natural surface cover within their city's boundaries had a stronger association between proximity to corridor and mange (Extended Data Fig. 2). Hence, our results suggest that, within cities, there is a higher likelihood of presence of coyotes with signs of sarcoptic mange near habitat connectivity corridors, in particular when there is an overall lower availability of natural surface cover in a city.

At the continental scale, we found contrasting results between coyote occupancy and mange occurrence among cities and their city-specific characteristics, in terms of urban density, and habitat availability and connectivity. While there was moderate evidence that coyote occupancy was lower in cities with higher overall human population density (0.81 probability of effect direction, $\beta^{\psi}_{\mathrm{POP}} = 0.69$; 90% BCI, −2.02 to 0.66), there was strong evidence that mange occurrence was higher in coyotes present in cities with a higher human population density (0.91 probability of effect direction, $\beta_{\omega} = 1.19$; 90% BCI, −0.28 to 2.69). In terms of habitat availability and connectivity, there was moderate evidence that coyote occupancy increased with the overall availability of natural habitat within a city (0.81 probability of effect direction, $\beta^{\psi}_{\mathrm{NAT}} = 0.65$; 90% BCI, −0.58 to 2.06) but no evidence of its association with the overall availability of movement corridors within a city ($\beta^{\psi}_{\mathrm{CQRR}} = 0.06$; 90% BCI, −0.87 to 0.90) nor the mean vegetation density of a city ($\beta^{\psi}_{\mathrm{NDVI}} = -0.10$; 90% BCI, −1.24 to 0.99; Extended Data Table 3). By contrast, there was very strong evidence that mange occurrence in coyotes decreased with a city's overall availability of movement corridors (0.97 probability of effect direction, $\beta_{\omega} = -1.34$; 90% BCI, −2.59 to −0.17) and its overall vegetation density (0.95 probability of effect direction, $\beta_{\omega} = -1.23$; 90% BCI, −2.38 to −0.01; Fig. 3a and Extended Data Table 3) but had no association with a city's total natural surface cover. These results suggest that a city with ten times more human population density (for example, 5.4 people km^2 versus 0.55 people km^2, following the range of values observed across cities included in this study) would have on average 29% lower coyote occupancy but 64% more mange occurrence in those coyotes (Fig. 3b). A city with ten times higher availability of natural areas (for example, cover proportion of 0.40 versus 0.04) would have 60% higher coyote occupancy while mange occurrence would not considerably change (Fig. 3b). A city with three times the mean vegetation density (for example, normalized difference vegetation index (NDVI) of 0.38 versus 0.12), or five times the availability of movement corridors (for example, cover proportion of 0.19 versus 0.04), would have 76% and 90% lower mange occurrence, respectively, with no considerable change in coyote occupancy (Fig. 3b).

https://doi.org/10.1038/s44284-026-00501-4

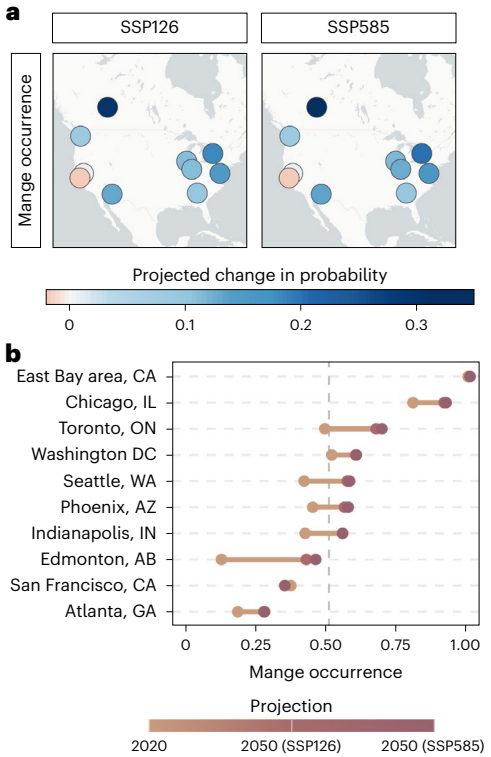

Fig. 4 | Disease forecast by 2050 following projected changes in urbanization density and climate. a, Geographic distribution of forecasted increases in mange occurrence across cities for the most-sustainable fossil fuel-consumption scenario SSP126 (left) and the least-sustainable fossil fuel-consumption scenario SSP585 (right) and the projected increase in urban population density (constant across future scenarios). **b**, Current (orange point) and forecasted increase in average mange occurrence (orange line) across cities following urban densification and climate change predicted for 2050 following SSP126 (light-red point) and SSP585 (dark-red point) future scenarios. AZ, Arizona; AB, Alberta; CA, California; IL, Illinois; IN, Indiana; ON, Ontario; WA, Washington. Map tiles in **a** from CartoDB © and OpenStreetMap contributors.

Hence, at a continental scale, our results suggest that while we may expect fewer coyotes in cities with denser urban centers, we can expect more of these to be affected by mange. By contrast, cities with more natural cover can expect a higher occupancy of coyotes, but if urban green areas in the city have high vegetation density and greater habitat connectivity, fewer of these coyotes will be affected by mange.

Climatic variables had a stronger effect on mange occurrence than on coyote occupancy (Extended Data Table 3). Mange occurrence had a 0.89 probability of being negatively associated with winter severity, measured as the proportion of the year below 0 °C (that is, chilling days, $\beta_\omega = -0.59$; 90% BCI, −1.41 to 0.22), and a 0.75 probability of being positively associated with higher relative humidity ($\beta_\omega = 0.36$; 90% BCI, −0.55 to 1.31; Fig. 3 and Extended Data Table 3). These results suggest that a city with more severe winters, for example, with a winter length and strength similar to Edmonton, Canada (highest chilling days in our study), would have on average 20% less mange occurrence than a city with a winter severity similar to Phoenix, Arizona (lowest chilling days in our study). Instead, in a city with 20% higher mean yearly humidity (for example, 74% versus 55%, highest versus lowest observed in our study), we expect on average 30% more mange occurrence.

With the current climate change and urban growth projections, our results suggest an increase in mange occurrence across cities by 2050. Following the projected climate change scenarios, with most-sustainable (SSP126) and least-sustainable (SSP585) economic activities (Extended Data Table 4), and the human population growth rate expected across cities, mange occurrence is expected to increase across nine of ten study cities by a median factor of 1.28 (SSP126) and 1.30 (SSP585), bringing seven out of ten cities to a mange occurrence of >0.50 (that is, mange occurrence at the majority of sites in the city; Fig. 4b). Cities with higher population growth rates and colder winters that are expected to become milder are likely to be the most affected by an increase in mange occurrence (Extended Data Table 4), for example, Edmonton (Alberta, Canada): a 3.4 times (SSP126) and 3.67 times (SSP585) increase. By contrast, cities at mid-continental latitudes, where winters are already mild, were the least affected by the future projections in mange occurrence, in particular those with stagnated population growth, for example, 0.94 times (SSP126 and SSP585) expected in San Francisco (California, USA).

Detection probabilities for both coyote occupancy and mange signs, when present, were high. There was a 0.95 probability of detecting a coyote at least once if coyotes were present (90% BCI, 0.87 to 0.99), given our average of 7.5 weeks sampled per survey. This detection probability was not associated with urbanization ($\beta_\rho = 0.02$; 90% BCI, −0.26 to 0.29) and was weakly associated with proximity to corridors ($\beta_\rho = 0.12$; 90% BCI, −0.17 to 0.42). The probability of detecting mange signs was 0.73 ($\beta_\rho = 0.81$; 90% BCI, 0.45 to 0.94), assuming our average of 12 coyote images per survey and average image quality. The detection of mange signs was most strongly impacted by the proportion of the body visible in an image ($\beta_\rho = 0.82$; 90% BCI, 0.48 to 1.16), whether an image was captured during daylight ($\beta_\rho = 0.75$; 90% BCI, −0.07 to 1.38) and whether an image had low levels of blurriness ($\beta_\rho = 0.42$; 90% BCI, −0.16 to 1.02). The high overall probability of detecting coyote (0.95) and mange (0.73) indicates that our study design provided sufficient information to quantify coyote occupancy and mange occurrence.

Discussion

We assessed the spatiotemporal differences in sarcoptic mange occurrence following local and continental processes, regarding urbanization, habitat connectivity and climate change (Table 1). At a local scale, we found that areas with a higher urbanization degree had a lower likelihood of coyote presence but a higher likelihood of mange occurrence. The presence of coyotes with mange was also more likely in areas of the city near movement pathways important for local habitat connectivity. At the continental scale, coyote occupancy was lower in denser cities with lower natural surface cover available but mange occurrence was higher (that is, present at more sites) in cities with denser human populations, lower vegetation density, fewer movement corridors between urban green areas and with climates characterized by warmer winters and higher humidity. On the basis of these among-city differences in mange occurrence, we forecast an increase in mange occurrence in nine out of ten of our study cities by 2050, regardless of the socioeconomic sustainability pathway scenario. Together, these results support our hypotheses that mange occurrence is either promoted or facilitated by urbanization, particularly in areas where host contact is increased via limited movement pathways, and in climates in which mite transmission likelihood is amplified via extended host and mite survival.

The diverging relationships we observed between urbanization and the occurrence of coyotes with and without signs of mange support previous studies and extend their generalizability beyond individual cities. While at a broad scale, coyotes are highly successful in urban areas[43], previous studies on coyote habitat use and occurrence using camera traps[44] and GPS collars[45] show that coyotes generally avoid areas with high human activity at a fine spatiotemporal scale[46–48]. Our results support the latter observations across all cities and suggest that coyotes are more likely to be present near movement pathways in most cities. In addition, our results suggest that coyotes, regardless of their disease status, are less likely to be widespread (that is, occupy fewer sites) in densely populated cities, and more likely to be widespread in urban areas with higher availability of natural areas.

In contrast to coyote occupancy patterns, we found a positive association between mange occurrence and urbanization within most study

https://doi.org/10.1038/s44284-026-00501-4

Table 1 | Covariates included within our multi-city, multistate autologistic occupancy model

Covariate	Description	Type	Included in			
			ψ	ω	ρ	γ
Urbanization	Principal component vector including building density, residential population density and natural surface area within 1-km buffer surrounding camera sites	Within-city	x	x	x	
Corridor proximity	Principal component vector including distance to predicted movement corridor and median normalized current density value within 1-km buffer surrounding camera sites. Values obtained from connectivity assessment using Omniscape	Within-city	x	x	x	
Urban population density	Residential population density within the city's boundaries	Among-city	x	x		
Vegetation density	Mean NDVI within the city's boundaries	Among-city	x	x		
Natural surface area	Total surface area covered by natural green areas within the city's boundaries	Among-city	x	x		
Corridor surface area	Total surface area covered by predicted movement corridors within the city's boundaries	Among-city	x	x		
Winter severity	Number of days below 0 °C (that is, chilling days), describes annual length characterized by freezing temperatures. Mean value across years between 2018 and 2023	Among-city	x	x		
Relative humidity	Annual mean relative humidity. Mean value across years between 2018 and 2023	Among-city	x	x		
Proportion of body captured	Proportion of the coyote body captured in an image	Image-level				x
Image time of day	Light conditions in which coyote image was captured	Image-level				x
Image distortion	Blur level of an image, characterized as binary using the mean distortion value as a threshold. Distortion estimated using computer vision	Image-level				x

The model jointly estimates four probabilities, all of which can be made a function of covariates through the logit-link: (1) the probability of coyote occupancy, mangy or otherwise (ψ); (2) the probability of mangy coyote given coyote presence (ω); (3) the probability of detecting coyote given their presence, mangy or otherwise (ρ); and (4) the probability of detecting a mangy coyote in a camera trap image given the presence of mangy coyote (γ).

cities, in particular in cities predominantly surrounded by agricultural land. The differences in association between urbanization degree and mange occurrence following the surrounding availability of natural habitat suggests coyotes with mange may be relegated to urban areas when alternative habitat or food resources are insufficient. Previous studies, in cities surrounded by a lower density of natural resources, have found that mange-infected coyotes were more urban and more reliant on residential food and shelter[13,15,49], in particular during winter[44], and were less likely to maintain territories than their healthy counterparts[14]. This suggests that diseased individuals are possibly being outcompeted and relegated to urban areas, in particular when the carrying capacity of the surrounding landscape is limited. Certain conditions may also amplify disease transmission in cities, probably leading to the higher mange occurrence we found in more densely populated cities. For example, previous studies suggest that a wider diet diversity in cities may prolong the survival of diseased coyotes[15], expanding their transmission potential. Carnivores residing in more urbanized areas may also be more susceptible to infection owing to exposure to rodenticides, as seen in bobcats *Lynx rufus*[26], or owing to diets lower in proteinaceous foods[15]. Coyotes in urban areas may also have a higher likelihood of parasite exposure, particularly if diseased hosts are exploiting supplemental resources in urban areas[44,49] when they are the weakest and most infective. Combined, our results at the local and continental scale further corroborate previous research highlighting the importance of urban areas on mange transmission, in particular as surrounded habitat is further lost with urban sprawl.

Habitat connectivity was associated with mange occurrence in diverse ways at different spatial scales. Within cities, mange occurrence was higher in areas near predicted movement corridors. Omnidirectional connectivity tools highlight these as areas where movement is concentrated given the local landscape configuration and its permeability to movement. This prediction was supported by our validation analysis, which showed a higher frequency of GPS-collared coyote movement along predicted movement corridors. Combined, our findings suggest that we can expect diseased individuals to use movement corridors more often than healthy coyotes, highlighting them as important transmission risk areas. Such association was stronger in cities with a lower availability of natural habitat within a city (Extended Data Fig. 2), suggesting that as connectivity corridors become more important for their movement within cities, transmission risk along these increases. Our results highlight the importance of urban landscape configuration on wildlife disease dynamics, supporting previous studies showcasing movement corridors as important for the transmission of other zoonotic diseases such as Lyme disease[50] and chronic wasting disease[51]. As habitat is further fragmented with urban growth, we can expect movement corridors to become more important for disease transmission.

However, relatively few studies have examined spatial patterns in wildlife disease across spatial scales[52], which can reveal contrasting outcomes, as it does in our study. At the local scale, we found diseased coyotes occurred more often in areas of the city closer to movement corridors. However, at the continental scale, we found mange occurrence was less widespread in cities with a higher availability of such movement corridors. Hence, while diseased coyotes may frequently use movement corridors and spread pathogens along movement corridors, a higher availability of corridors does not increase the likelihood of disease transmission. Higher habitat connectivity at the landscape scale, by providing a rich network of many movement pathways, decreases the encounter likelihood among hosts in each individual corridor. This pattern at the continental scale challenges the common perception that highly-connected landscapes will necessarily promote pathogen spread[53] and emphasizes the need to study the relationships among habitat connectivity and disease risk across different landscapes and scales.

Disentangling the contribution of habitat availability and connectivity to ecological responses is challenging[54,55]. However, in our study, the consideration of three landscape covariates concerning habitat availability and connectivity for both coyote occupancy and mange occurrence helps to disentangle this relationship. At the continental scale, we found an association between the quantity of natural surface cover in cities with increased coyote occupancy, while we found no association with mange occurrence. Instead, we found an association between decreased mange occurrence and a city's availability of movement corridors and its overall vegetation density, regardless of the quantity of delimited natural areas available. This suggests that differences in habitat connectivity in terms of the number of movement pathways between green areas and the overall permeability of a city's landscape to animal movement were key for mange occurrence, more

so than the overall presence of natural areas. These results emphasize the role of landscape configuration on wildlife disease occurrence, in particular in fragmented landscapes, such as cities. This is corroborated by our local scale results, which suggest movement corridors are potentially high transmission areas strongly used by diseased coyotes. Hence, if more unobstructed corridors were available in a region with the same overall amount of natural areas, we would expect less concentration of movement into these corridors and potentially lower rates of disease transmission. Furthermore, our results emphasize the importance of vegetation within the urban matrix (for example, gardens, yards and road verges) in diversifying animal movement routes and providing cover, further reducing the risk of host encounters and disease transmission. Habitat connectivity may become increasingly important for territorial species, whereby disease impacts a host's ability to defend territories and find resources. In these cases, individuals incapable of defending territories[15] may become more mobile, increasing their use of movement pathways and encountering more susceptible individuals, in particular when movement routes are limited. In such cases, a stronger reliance on anthropogenic resources and a higher need for large-scale movement patterns could act in tandem with habitat connectivity loss to intensify disease transmission.

Cities with milder winters and higher relative humidity had a higher likelihood of mange occurrence, probably in part owing to mite and infected-host physiology. Milder winters extend the lifespan of both off-host mites and diseased hosts. The survival of the latter is reduced in areas with severe winter temperatures (−30 to −40 °C)[56] and mange-associated mortality events are more frequent during the winter in colder cities, such as Chicago (Illinois, USA)[57]. Hence, stronger winters can reduce the time span in which diseased hosts can encounter susceptible individuals. Off-host mite survival is also reduced in more severe winters, as mites cannot survive in snow[58] and their off-host lifespan increases to up to 19 days as temperature and relative humidity increases[33,59], which is typical of Southeastern cities such as Atlanta (Georgia, USA). *S. scabiei* mites remain infective for one- to two-thirds of their off-host survival period; therefore, environmental conditions are a strong determinant of indirect transmission. Climate variables are probably the most important for susceptible species using denning sites, such as coyotes and foxes, and for cities where green space availability is limited, increasing intra- and interspecific home-range overlap and the re-use of denning sites[60]. Similarly, climate variables may also be important for vector-transmitted diseases, where disease success also depends on invertebrate survival[61].

On the basis of future climate and development projections, we forecasted an increase in mange occurrence in most study cities, whereby milder winters associated with climate change acts in tandem with expected population growth. Hence, densifying cities at higher latitudes, where winters have been forecasted to become warmer, will be most impacted by climate change. This is probably because colder and longer winters may limit the survival of diseased hosts and off-host mites, and this protective factor will be lost in the current prospective climate trajectory. In addition to climate, higher projected population growth may further reduce foraging areas available to coyotes following their human avoidance patterns, increasing the spatial overlap and transmission risk between susceptible and diseased coyotes. It is important to consider that our projections do not consider urban sprawl and land-use conversion, which generally reduce habitat availability and connectivity, which based on our results, would further intensify the expected increase in mange occurrence.

Our work focused on sarcoptic mange given its distinctive visible signs of infection, which enabled us to use a multi-city network of camera traps following a standardized study design. However, this approach does not incorporate other health metrics, limiting our inferences about infection severity or host demographics. Future studies could incorporate host or environmental sampling in the field to complement camera monitoring[62]. Such studies could also incorporate other aspects of disease ecology such as host community structure and interspecies contact networks. Future work could also take advantage of the growing use of computer vision to automate image tagging from wildlife camera trapping[63] to facilitate large-scale studies and account for multiple aspects of image quality. While we focused on sarcoptic mange, additional studies could use camera traps to monitor other wildlife diseases with visible signs, such as pox viruses in many mammal and bird species[64], Leishmaniasis in several mammalian orders[65] and visible cancer signs in Tasmanian devils[66]. In combination, technological advancements with cameras, image processing and One Health collaborations between veterinarians and ecologists can increase the scale of disease monitoring and our understanding of disease dynamics with global change.

Conclusion

This work integrates the analysis of disease distribution at multiple spatial scales, providing more robust and generalizable patterns in disease occurrence. Our results suggest that the prevalence of a panzootic parasite—sarcoptic mange—increases with urbanization, especially as surrounding habitat is lost to agriculture, with connectivity loss between urban green areas and with warmer, more humid climates. As such, projected trends in urban development and climate change are expected to exacerbate disease occurrence in urban areas. As the world becomes more urbanized, it is imperative to preserve diverse travel routes for wildlife to reduce contact rates, manage anthropogenic food sources that might aggregate individuals and mitigate climate change to protect biodiversity and human health from wildlife disease risk[67]. Cities with accelerated winter warming are particularly at risk, necessitating enhanced monitoring. Large-scale monitoring efforts using passive non-invasive tools such as camera traps will help predict such high-risk contexts to protect wildlife, domestic animals and human health on our urbanizing and warming planet.

Methods

Data collection

We derived detection/non-detection data from images of coyotes collected using camera traps located within ten cities, across the USA (eight) and Canada (two). The camera traps were placed following the UWIN systematic sampling design, whereby camera traps are placed in urban green spaces along an urbanization gradient, either within three 2-km-wide transects or on a grid-like matrix, for four fixed seasons throughout each year[68]. The minimum distance between camera traps was 1 km to reduce spatial autocorrelation. Detection histories for each site, and primary sampling period, were generated using sampling week as the secondary sampling period. Temporal autocorrelation was accounted for within the autologistic occupancy model through the inclusion of a first-order autoregressive term added to the two occupancy logit-linear predictors[8]. We included a minimum of one full year of sampling for each city between 2019 and 2023, that is, a minimum of four contiguous seasons of sampling (max of 10 seasons, mean of 4.3 seasons) with a median of 8 weeks per season. Except for East Bay area, California, which only had three seasons across 36 sites. The median number of unique camera-trapping sites per city was 39 (min of 25, max of 112; Extended Data Table 1). Coyotes across sites were identified by trained experts and validated by ecologists with experience identifying local terrestrial mammals.

Mange detection

We analyzed each coyote image for signs consistent with mange, which included alopecia—that is, patches of hair loss—or skin crusts[69]. An initial set of these were verified by a veterinarian, which served to train observers. For each image, we estimated the proportion of body visible, the proportion of body visible with mange signs and the severity of symptoms categorized into mild, moderate or severe. In addition, using computer vision, followed by manual verification, we assessed

whether the image was captured during daytime using Timelapse2[70], on the basis of pixel darkness, and whether the image was blurred by computing the Laplacian variance of the image, using the Laplacian().var() function from the OpenCV library[71]. For the latter, we assigned the image to a binary category (blurry/non-blurry) following the median Laplacian variance across images as a threshold[8]. We used these variables for the within-image state of the model, where the imperfect detection of mange is considered for the mange occupancy estimates.

Statistical analysis

We extended the multistate autologistic occupancy model described by Murray et al.[8], which uses a Bayesian framework to jointly estimate coyote occurrence and the conditional distribution of coyote with visible signs of mange. Specifically, this model uses a set of conditional binomials to estimate the probability of coyote occupancy, mangy or otherwise (ψ), as well as the conditional probability of mange occurrence given coyote presence (ω). These probabilities have their own observational models. For coyote occupancy, we account for site- and city-level variation in detecting coyotes, mangy or otherwise, given their presence at a site (ρ). For mange occupancy we account for image-level variation in detecting mange on a coyote given the presence of mangy coyote at a site (γ). All four of these estimated probabilities were made a function of covariates using the logit-link (Table 1), and the sections below detail how we collected and scaled our covariates for analysis. It is important to note that, as with the majority of camera-trap occupancy studies, the parameters estimated from our model should be interpreted as habitat use instead of true occupancy, as violations of site closure are possible[72]. See Murray et al.[8] for a more thorough description of this class of model.

To extend this model, we incorporated city-level random intercept and slope terms into the parameter hierarchy for all model intercepts and within-city slope terms (that is, response to urbanization and proximity to corridors). All random effects were assigned their own normal priors with an associated among-city average parameter and standard deviation term. For example, the parameter hierarchy for the intercept of the coyote occupancy, mangy or otherwise, at c in $1,\ldots,C$ cities was $\beta^{\psi}_{0,c} \sim \text{Normal}(\beta^{\psi}_{0}, \sigma^{\psi}_{0})$, where $\beta^{\psi}_{0} \sim \text{Logistic}(0,1)$ and $\sigma^{\psi}_{0} \sim \text{Inv.Gamma}(1,1)$. Our model also included six among-city covariates that varied by city rather than sites within each city. As these parameters are shared across cities, we assigned them uninformative logistic(0,1) priors. See the sections below for how covariate data were collected and scaled for analysis.

Spatial variables

Urbanization. We defined urbanization as an increase in built environment and human presence and a decrease in habitat availability in terms of natural vegetation. For this, we included the values within 1 km of each camera trap site, of (1) the mean value of total surface covered by buildings (that is, roofed structures) per cell of 10-m resolution[73]; (2) mean human population density, expressed as the number of people per cell of 100-m resolution[74]; and (3) total surface area composed of natural vegetation (forest and heterogeneous vegetation cover from the OSM-enhanced land cover map[75]). The first two were derived from Sentinel-2 composite (2018) by the Global Human Settlement[76] and the latter was derived from OpenStreetMap and the European Space Agency (ESA) World cover following Gelmi-Candusso et al.[75]. With the site-specific values of these three landscape components, scaled and centered to each city's mean, we defined the level of urbanization using the first component of a PCA, which explained 77.3% of the variation in the data across all sites.

Habitat connectivity. We assessed the importance of the area surrounding a site in terms of local habitat connectivity using the normalized current density values estimated with Omniscape[40,77]. Current density estimates the probability of animal movement across a study area. The highest current-density values indicate areas where animal movement is predicted to be concentrated, moderate current-density areas indicate areas with a variety of movement pathways available (diffused flow zone) and low current-density values indicate areas where movement likelihood is predicted to be low, given high interference of the landscape[39,78] (Extended Data Figs. 3 and 4). This assessment of current flow is based on a resistance map, where each cell is characterized in terms of resistance to movement. These resistance values were estimated using the mean values of population density, built surface area, described above, and the NDVI, and the relationship between these components was defined through a sensitivity analysis. To maintain comparability between cities, these resistance layers were normalized to a 0–100 scale using their maximum value across cities. In addition to these layers, we included waterways and the road and highway network derived from OpenStreetMap[75]. To estimate resistance values for each cell, we combined all layers with a weighted sum, whereby population density and built surface area increased resistance by a weight of one, NDVI reduced resistance by a weight of three, following previous studies estimating the relative selection strengths of these variables from GPS collared coyotes[79], and roads increased resistance by a weight defined by the surrounding human population density. To these resistance values, we overlaid the streams, lakes and oceans which we considered as maximum resistance. As the presence of large areas of high resistance can create artifacts in terms of current flow[80], we ran a sensitivity analysis comparing the use of high-resistance values for water bodies, a neutral set of resistance values and the use of raw values instead of normalized current density values, validated using GPS-collared data, which suggested that using water bodies with high resistance better reflects coyote movement patterns (Supplementary Section 2). To understand how the configuration of habitats and resistance interact to shape movement networks, Omniscape requires a second input to define the source strength values of each pixel. Here, we used the tool's option to derive the source strength from the inverse of the resistance values, such that the most 'natural' areas acted as the highest sources within the moving window. We did this to better reflect the opportunistic and adaptable nature of coyotes across cities in different ecoregions and emulate the natural adaptability of coyotes, as they select areas where to shelter and forage on the basis of the land available in their vicinity. We used Omniscape v0.6.2 with a window radius of ~10 km (that is, 333 cells of 30 × 30 m in resolution), emulating maximum net displacement observed for coyotes within 72 h[81], and a block size of ~1 km^2 (that is, 33 cells), through an iterative solver using conjugate gradient with an algebraic multigrid preconditioner (CG + AMG), which we ran locally parallelized on 16 threads. We chose to use the normalized current flow product rather than the 'raw' cumulative current output. This output uses a null model of current flow without resistance to help identify areas where current density has become elevated in response to resistance, including in places where the overall density of sources (natural areas) is low, a common situation in urban areas. The usage frequency of cells with a higher current density, as predicted by the connectivity model, was validated using data from GPS-collared coyotes in Atlanta (Georgia, USA) and Toronto (Ontario, Canada) and a step-selection function with current density and resistance as a covariate (Supplementary Section 1).

With the normalized current density values from Omniscape, we derived site-specific levels of importance in terms of habitat connectivity through a PCA. In the PCA we included the (1) mean current density within a 1-km buffer of each site, to reflect the availability of movement pathways around the site, as mid-to-high overall current density values would suggest a site located in a position with redundant movement pathways, while the lowest values would suggest a site in a position of lower movement likelihood and (2) the distance to the nearest predicted movement corridor, defined as the top 10% of values of current density within each study area (after masking water bodies)[42], where we would expect concentrated movement flow. We scaled and centered both components to each city's mean value. We defined proximity to areas key for habitat connectivity using the first

component of a PCA, which explained 64.6% of the variation in the data across all sites, whereby sites along the axis had higher mean current density and were closer to movement corridors.

Among-city variables. For the among-city variables, we measured within the municipal city boundaries of each study area the mean value of each of the covariates included in the PCAs explained above. We used only the areas within urban boundaries, that is, cells characterized as urban center or urban cluster by the Global Human Settlement[76], as opposed to the full study area, to minimize bias introduced in the summary statistics by the surrounding non-urban landscape, which varied in size and type across study areas. In addition, to render the model more robust, we eliminated among-city covariates that were redundant and resulted in the same effect direction. The final spatial covariates included in the model were (1) mean human population density, (2) mean normalized vegetation density, (3) total natural vegetation surface area and (4) total movement corridor surface area, as described above. Covariates eliminated from the analysis included mean built-surface area, which resulted in the same effect directionality as population density but with higher variability, and mean current density within the city boundary, which resulted in an equivalent effect of total movement corridor surface area. We did not use PCA vectors as among-city covariates given the low sample number of cities, which was insufficient to estimate a reliable eigenvector to use as a covariate.

Climate variables

We included climate covariates that would account for the abiotic factors determining vertebrate host survival and off-host survival of mites. These included chilling days and relative humidity. Chilling days estimate the proportion of time within a year below 0 °C and account for winter length and temperature, which can affect both host and off-host mite survival[57,58]. Relative humidity accounts for the degree of saturation of the air with water vapor relative to the temperature, which can affect off-host mite survival[33]. These values were obtained from the ClimateNA v6.40b software package[82] using the function ClimateNAr() from the ClimateNAr package[83] for the years 2018–2023, for which we estimated the 5-year mean of each city.

Priors and model run specification

To fit the multistate autologistic occupancy model, we used JAGS v 4.3.0 in R v 4.4.1 via the runjags R package[84–86]. Following a 1,000-step adaptation phase and a 25,000-step burn-in phase, we sampled six chains for 200,000 steps each—thinning by 4—which resulted in 300,000 posterior samples. To assess model convergence, we calculated Gelmin–Rubin diagnostics for all model parameters and determined if they were all less than 1.10 (ref. 87). We reported evidence of effect in two ways. First, we calculated the probability of effect direction by determining the proportion of a model coefficient's marginal posterior that was greater or less than 0, depending on the direction of the effect. As marginal posteriors are probability distributions, this metric provides evidence on how certain we are that a given effect is either negative or positive, thereby reducing the need to use binary thresholds to determine significance (for example, credible intervals that overlap zero). To help with interpretation, we described associations with a probability >0.90 of the posterior values being positive or negative as a strong effect and those with a probability <0.70 as weak evidence of an effect; associations in between were considered as having a moderate effect. These labels are meant to summarize patterns and are not strict decision rules. To illustrate parameter uncertainty, we calculated 90% BCIs, which are more computationally stable than 95% BCIs.

Future projections

We predicted mange occupancy with our multistate occupancy model by predicting mange occupancy on climate projections and urban growth for the year 2050. Climate scenarios included the SSP126 and SSP585, which consider a sustainable future where fossil fuel exploitation is reduced and a future where fossil fuel extraction is unrestricted[88], respectively. Projections on urban densification included the local urban population growth rate estimated for a study area's urban area sourced from state, municipal agencies or local academic institutions (Extended Data Table 4).

Reporting summary

Further information on research design is available in the Nature Portfolio Reporting Summary linked to this article.

Data availability

Data are available via GitHub at https://github.com/tgelmi-candusso/CTwildlifedisease and via Zenodo at https://doi.org/10.5281/zenodo.17210906 (ref. 89).

Code availability

Code is available via GitHub at https://github.com/tgelmi-candusso/CTwildlifedisease and via Zenodo at https://doi.org/10.5281/zenodo.17210906 (ref. 89).

References

1. Thieltges, D. W. et al. Integrating climate change, biological invasions, and infectious wildlife diseases. *Front. Ecol. Environ.* **23**, e2849 (2025).
2. Hassell, J. M., Begon, M., Ward, M. J. & Fèvre, E. M. Urbanization and disease emergence: dynamics at the wildlife–livestock–human interface. *Trends Ecol. Evol.* **32**, 55–67 (2017).
3. Biswas, J. K., Mukherjee, P., Vithanage, M. & Prasad, M. N. V. in *One Health* 19–37 (eds Vithanage, M. & Prasad, M. N. V.) (John Wiley, 2023); https://doi.org/10.1002/9781119867333.ch2
4. Cohen, J. M., Sauer, E. L., Santiago, O., Spencer, S. & Rohr, J. R. Divergent impacts of warming weather on wildlife disease risk across climates. *Science* **370**, eabb1702 (2020).
5. Bradley, C. A. & Altizer, S. Urbanization and the ecology of wildlife diseases. *Trends Ecol. Evol.* **22**, 95–102 (2007).
6. Murray, M. H. et al. Multicity research networks are needed to address global One Health challenges. *BioScience* biaf106 https://doi.org/10.1093/biosci/biaf106 (2025).
7. Magle, S. B. et al. Advancing urban wildlife research through a multi-city collaboration. *Front. Ecol. Environ.* **17**, 232–239 (2019).
8. Murray, M. H., Fidino, M., Lehrer, E. W., Simonis, J. L. & Magle, S. B. A multi-state occupancy model to non-invasively monitor visible signs of wildlife health with camera traps that accounts for image quality. *J. Anim. Ecol.* **90**, 1973–1984 (2021).
9. Escobar, L. E. et al. Sarcoptic mange: an emerging panzootic in wildlife. *Transbound. Emerg. Dis.* **69**, 927–942 (2022).
10. Martin, A. M., Burridge, C. P., Ingram, J., Fraser, T. A. & Carver, S. Invasive pathogen drives host population collapse: effects of a travelling wave of sarcoptic mange on bare-nosed wombats. *J. Appl. Ecol.* **55**, 331–341 (2018).
11. Matsuyama, R., Kido, N. & Omori, R. Estimating the impact of sarcoptic mange epidemic on the population size of wild raccoon dogs (*Nyctereutes procyonoides*) from wildlife rescue data. *Int. J. Parasitol. Parasites Wildl.* **25**, 101010 (2024).
12. Cypher, B. L. et al. Sarcoptic mange in endangered kit foxes (*Vulpes macrotis mutica*): case histories, diagnoses, and implications for conservation. *J. Wildl. Dis.* **53**, 46–53 (2017).
13. Murray, M. H., Edwards, M. A., Abercrombie, B. & St. Clair, C. C. Poor health is associated with use of anthropogenic resources in an urban carnivore. *Proc. R. Soc. B* **282**, 20150009 (2015).
14. Reddell, C. D., Roemer, G. W., Delaney, D. K., Karish, T. & Cain, J. W. Anthropogenic subsidies influence resource use during a mange epizootic in a desert coyote population. *Oecologia* **201**, 435–447 (2023).

15. Murray, M. et al. Greater consumption of protein-poor anthropogenic food by urban relative to rural coyotes increases diet breadth and potential for human–wildlife conflict. *Ecography* **38**, 1235–1242 (2015).
16. Bandi, K. M. & Saikumar, C. Sarcoptic mange: a zoonotic ectoparasitic skin disease. *J. Clin. Diagn. Res.* **7**, 156–157 (2013).
17. Guillot, J. et al. in *Scabies* (eds Fischer, K. & Chosidow, O.) 313–343 (Springer, 2023); https://doi.org/10.1007/978-3-031-26070-4_23
18. Zinsstag, J., Schelling, E., Waltner-Toews, D. & Tanner, M. From 'one medicine' to 'one health' and systemic approaches to health and well-being. *Prev. Vet. Med.* **101**, 148–156 (2011).
19. Kraabøl, M., Gundersen, V., Fangel, K. & Olstad, K. The taxonomy, life cycle and pathology of *Sarcoptes scabiei* and *Notoedres cati* (Acarina, Sarcoptidae): a review in a Fennoscandian wildlife perspective. *Fauna Norv.* **35**, 21–33 (2015).
20. Parsons, A. W. et al. Urbanization focuses carnivore activity in remaining natural habitats, increasing species interactions. *J. Appl. Ecol.* **56**, 1894–1904 (2019).
21. Saito, M. U. & Sonoda, Y. Symptomatic raccoon dogs and sarcoptic mange along an urban gradient. *EcoHealth* **14**, 318–328 (2017).
22. Foley, P. et al. Spatio-temporal and transmission dynamics of sarcoptic mange in an endangered New World kit fox. *PLoS ONE* **18**, e0280283 (2023).
23. Carricondo-Sanchez, D., Odden, M., Linnell, J. D. C. & Odden, J. The range of the mange: spatiotemporal patterns of sarcoptic mange in red foxes (*Vulpes vulpes*) as revealed by camera trapping. *PLoS ONE* **12**, e0176200 (2017).
24. Scott, D. M. et al. Spatial distribution of sarcoptic mange (*Sarcoptes scabiei*) in urban foxes (*Vulpes vulpes*) in Great Britain as determined by citizen science. *Urban Ecosyst.* **23**, 1127–1140 (2020).
25. Reddell, C. D., Abadi, F., Delaney, D. K., Cain, J. W. & Roemer, G. W. Urbanization's influence on the distribution of mange in a carnivore revealed with multistate occupancy models. *Oecologia* **195**, 105–116 (2021).
26. Serieys, L. E. K. et al. Urbanization and anticoagulant poisons promote immune dysfunction in bobcats. *Proc. Biol. Sci.* **285**, 20172533 (2018).
27. Riley, S. P. D., Serieys, L. E. K. & Moriarty, J. G. Infectious in *Urban Wildlife Conservation: Theory and Practice* (eds McCleery, R. A. et al.) 175–215 (Springer, 2014); https://doi.org/10.1007/978-1-4899-7500-3_10
28. Niedringhaus, K. D., Brown, J. D., Sweeley, K. M. & Yabsley, M. J. A review of sarcoptic mange in North American wildlife. *Int. J. Parasitol. Parasites Wildl.* **9**, 285–297 (2019).
29. Devenish-Nelson, E. S., Richards, S. A., Harris, S., Soulsbury, C. & Stephens, P. A. Demonstrating frequency-dependent transmission of sarcoptic mange in red foxes. *Biol. Lett.* **10**, 20140524 (2014).
30. Dimitrov, N., Gelmi-Candusso, T. A., Krkosek, M. & Fortin, M.-J. The effects of fox movement and landscape heterogeneity on the spread of sarcoptic mange in urban settings. Preprint at *bioRxiv* https://doi.org/10.64898/2026.06.24.734291 (2026).
31. Lilly, M. V. et al. Functional connectivity for white-tailed deer drives the distribution of tick-borne pathogens in a highly urbanized setting. *Landsc. Ecol.* **40**, 87 (2025).
32. Cross, P. C. et al. Energetic costs of mange in wolves estimated from infrared thermography. *Ecology* **97**, 1938–1948 (2016).
33. Arlian, L. G., Vyszenski-Moher, D. L. & Pole, M. J. Survival of adults and development stages of *Sarcoptes scabiei* var. *canis* when off the host. *Exp. Appl. Acarol.* **6**, 181–187 (1989).
34. Loredo, A. I., Rudd, J. L., Foley, J. E., Clifford, D. L. & Cypher, B. L. Climatic suitability of San Joaquin kit fox (*Vulpes macrotis mutia*) dens for sarcoptic mange (*Sarcoptes scabiei*) transmission. *J. Wildl. Dis.* **56**, 126–133 (2019).
35. Ringwaldt, E. M. et al. Host, environment, and anthropogenic factors drive landscape dynamics of an environmentally transmitted pathogen: sarcoptic mange in the bare-nosed wombat. *J. Anim. Ecol.* **92**, 1786–1801 (2023).
36. Li, G. et al. Global impacts of future urban expansion on terrestrial vertebrate diversity. *Nat. Commun.* **13**, 1628–12 (2022).
37. Wang, J. et al. Changing lengths of the four seasons by global warming. *Geophys. Res. Lett.* **48**, e2020GL091753 (2021).
38. Riahi, K. et al. The shared socioeconomic pathways and their energy, land use, and greenhouse gas emissions implications: an overview. *Glob. Environ. Change* **42**, 153–168 (2017).
39. McRae, B. H., Dickson, B. G., Keitt, T. H. & Shah, V. B. Using circuit theory to model connectivity in ecology, evolution, and conservation. *Ecology* **89**, 2712–2724 (2008).
40. Landau, V. A., Shah, V. B., Anantharaman, R. & Hall, K. R. Omniscape.jl: software to compute omnidirectional landscape connectivity. *J. Open Source Softw.* **6**, 2829 (2021).
41. Pither, R., O'Brien, P., Brennan, A., Hirsh-Pearson, K. & Bowman, J. Predicting areas important for ecological connectivity throughout Canada. *PLoS ONE* **18**, e0281980 (2023).
42. Gelmi-Candusso, T. A., Chin, A. T. M., Ruppert, J. L. W. & Fortin, M.-J. Urban planning for wildlife connectivity: a multispecies assessment of urban sprawl and SLOSS renaturalization strategies. *J. Appl. Ecol.* **62**, 1007–1023 (2025).
43. Poessel, S. A., Gese, E. M. & Young, J. K. Environmental factors influencing the occurrence of coyotes and conflicts in urban areas. *Landsc. Urban Plan.* **157**, 259–269 (2017).
44. Murray, M. H. & St. Clair, C. C. Predictable features attract urban coyotes to residential yards. *J. Wildl. Manage.* **81**, 593–600 (2017).
45. Van Scoyoc, A., Calhoun, K. L. & Brashares, J. S. Using multiple scales of movement to highlight risk–reward strategies of coyotes (*Canis latrans*) in mixed-use landscapes. *Ecosphere* **15**, e4977 (2024).
46. Gehrt, S. D., Anchor, C. & White, L. A. Home range and landscape use of coyotes in a metropolitan landscape: conflict or coexistence?. *J. Mammal.* **90**, 1045–1057 (2009).
47. Nickel, B. A., Suraci, J. P., Allen, M. L. & Wilmers, C. C. Human presence and human footprint have non-equivalent effects on wildlife spatiotemporal habitat use. *Biol. Conserv.* **241**, 108383 (2020).
48. Devarajan, K. et al. When the wild things are: defining mammalian diel activity and plasticity. *Sci. Adv.* **11**, eado3843 (2025).
49. Murray, M. H., Hill, J., Whyte, P. & St Clair, C. C. Urban compost attracts coyotes, contains toxins, and may promote disease in urban-adapted wildlife. *Ecohealth* **13**, 285–292 (2016).
50. Watts, A. G. et al. Host functional connectivity and the spread potential of Lyme disease. *Landscape Ecol.* **33**, 1925–1938 (2018).
51. Nobert, B. R., Merrill, E. H., Pybus, M. J., Bollinger, T. K. & Hwang, Y. T. Landscape connectivity predicts chronic wasting disease risk in Canada. *J. Appl. Ecol.* **53**, 1450–1459 (2016).
52. Albery, G. F., Sweeny, A. R., Becker, D. J. & Bansal, S. Fine-scale spatial patterns of wildlife disease are common and understudied. *Funct. Ecol.* **36**, 214–225 (2022).
53. McCallum, H. & Dobson, A. Disease, habitat fragmentation and conservation. *Proc. R. Soc. Lond. B* **269**, 2041–2049 (2002).
54. Lindenmayer, D. B. et al. Habitat amount versus connectivity: an empirical study of bird responses. *Biol. Conserv.* **241**, 108377 (2020).
55. Lambin, E. F., Tran, A., Vanwambeke, S. O., Linard, C. & Soti, V. Pathogenic landscapes: interactions between land, people, disease vectors, and their animal hosts. *Int. J. Health Geogr.* **9**, 54 (2010).
56. Bornstein, S., Mörner, T. & Samuel, W. M. in *Parasitic Diseases of Wild Mammals* (eds Samuel, W. M. et al.) 107–119 (Wiley, 2001); https://doi.org/10.1002/9780470377000.ch5

57. Wilson, E. C. The dynamics of sarcoptic mange in an urban coyote (*Canis latrans*) population. (Ohio State Univ., 2012).
58. Niedringhaus, K. D., Brown, J. D., Ternent, M. A., Peltier, S. K. & Yabsley, M. J. Effects of temperature on the survival of *Sarcoptes scabiei* of black bear (*Ursus americanus*) origin. *Parasitol. Res.* **118**, 2767–2772 (2019).
59. Pandey, A. et al. The influence of social and spatial processes on the epidemiology of environmentally transmitted pathogens in wildlife: implications for management. *Philos. Trans. R. Soc. B* **379**, 20220532 (2024).
60. Montecino-Latorre, D. et al. Assessing the role of dens in the spread, establishment and persistence of sarcoptic mange in an endangered canid. *Epidemics* **27**, 28–40 (2019).
61. de Souza, W. M. & Weaver, S. C. Effects of climate change and human activities on vector-borne diseases. *Nat. Rev. Microbiol.* **22**, 476–491 (2024).
62. Barroso, P. et al. Using integrated wildlife monitoring to prevent future pandemics through One Health approach. *One Health* **16**, 100479 (2023).
63. Ringwaldt, E. M., Buettel, J. C., Carver, S. & Brook, B. W. Epidemiological dynamics of a visually apparent disease: camera trapping and machine-learning applied to rumpwear in the common brushtail possum. *Integr. Zool.* **21**, 116–128 (2026).
64. Mohamed, R. I. et al. Molecular and pathological screening of the current circulation of fowlpox and pigeon pox virus in backyard birds. *Poult. Sci.* **103**, 104249 (2024).
65. López, M. et al. Measuring spatial co-occurrences of species potentially involved in Leishmania transmission cycles through a predictive and fieldwork approach. *Sci. Rep.* **11**, 6789 (2021).
66. Thalmann, S., Wise, P. & Huxtable, S. in *Camera Trapping* 27–35 (CSIRO Publishing, 2014).
67. Tzoulas, K. et al. Promoting ecosystem and human health in urban areas using Green Infrastructure: a literature review. *Landsc. Urban Plan.* **81**, 167–178 (2007).
68. Fidino, M. et al. Landscape-scale differences among cities alter common species' responses to urbanization. *Ecol. Appl.* **31**, e02253 (2021).
69. Pence, D. B., Windberg, L. A., Pence, B. C. & Sprowls, R. The epizootiology and pathology of sarcoptic mange in coyotes, *Canis latrans*, from South Texas. *J. Parasitol.* **69**, 1100–1115 (1983).
70. Greenberg, S., Godin, T. & Whittington, J. Design patterns for wildlife-related camera trap image analysis. *Ecol. Evol.* **9**, 13706–13730 (2019).
71. Bradski, G. The OpenCV Library. *Dr. Dobb's J. Softw. Tools* **25**, 120–125 (2000).
72. in *Occupancy Estimation and Modeling (Second Edition)* (eds MacKenzie, D. I. et al.) i–iii (Academic Press, 2018); https://doi.org/10.1016/B978-0-12-407197-1.00023-5
73. Pesaresi, M. & Politis, P. GHS-BUILT-S R2023A - GHS built-up surface grid, derived from Sentinel2 composite and Landsat, multitemporal (1975–2030). *European Commission* https://doi.org/10.2905/9F06F36F-4B11-47EC-ABB0-4F8B7B1D72EA (2023).
74. Schiavina, M., Freire, S., Carioli, A. & MacManus, K. GHS-POP R2023A - GHS population grid multitemporal (1975–2030). *European Commission* https://doi.org/10.2905/2FF68A52-5B5B-4A22-8F40-C41DA8332CFE (2023).
75. Gelmi-Candusso, T. A. et al. Leveraging open-source geographic databases to enhance the representation of landscape heterogeneity in ecological models. *Ecol. Evol.* **14**, e70402 (2024).
76. *GHSL Data Package 2023* (Publications Office, 2023); https://doi.org/10.2760/20212
77. McRae, B. et al. *Conserving Nature's Stage: Mapping Omnidirectional Connectivity for Resilient Terrestrial Landscapes in the Pacific Northwest* (Nature Conservancy, 2016); https://doi.org/10.13140/RG.2.1.4158.6166
78. Pelletier, D. et al. Applying circuit theory for corridor expansion and management at regional scales: tiling, pinch points, and omnidirectional connectivity. *PLoS ONE* **9**, e84135 (2014).
79. Gelmi-Candusso, T. A. et al. Dynamic connectivity assessment for a terrestrial predator in a metropolitan region. *Front. Ecol. Environ.* **22**, e2633 https://doi.org/10.1002/fee.2633 (2024).
80. Clark, M., Anderson, J., Anderson, M. G., Hall, K. R. & Poor, E. E. Wade carefully: water parametrization in structural landscape connectivity modeling. *Landsc. Ecol.* **40**, 117 (2025).
81. Gelmi-Candusso, T. A., Wheeldon, T. J., Patterson, B. R. & Fortin, M.-J. The effect of urbanization and behavioral factors on coyote net displacement and its implications for seed dispersal. *Urban Ecosyst.* https://doi.org/10.1007/s11252-023-01460-7 (2023).
82. Wang, T., Hamann, A., Spittlehouse, D. & Carroll, C. Locally downscaled and spatially customizable climate data for historical and future periods for North America. *PLoS ONE* **11**, e0156720 (2016).
83. Wang, T., Hamann, A., Spittlehouse, D. L. & Carroll, C. Locally downscaled and spatially customizable climate data for historical and future periods for North America. *PLoS ONE* **11**, e0156720 (2016).
84. R Core Team. *R: A Language and Environment for Statistical Computing* http://www.R-project.org/ (R Foundation for Statistical Computing, 2024).
85. Plummer, M. JAGS: a program for analysis of Bayesian graphical models using Gibbs sampling. In *Proc. 3rd International Workshop on Distributed Statistical Computing* **124**, 1–10 (2003).
86. Denwood, M. J. runjags: an R package providing interface utilities, model templates, parallel computing methods and additional distributions for MCMC models in JAGS. *J. Stat. Softw.* **71**, 1–25 (2016).
87. Gelman, A., Carlin, J. B., Stern, H. S., Rubin, D. B. Bayesian Data Analysis (Chapman and Hall/CRC, 1995).
88. O'Neill, B. C. et al. A new scenario framework for climate change research: the concept of shared socioeconomic pathways. *Clim. Change* **122**, 387–400 (2014).
89. Gelmi-Candusso, T. et al. Wildlife disease occurrence increases with urbanization, habitat connectivity loss, and climate change. *Zenodo* https://doi.org/10.5281/zenodo.17210906 (2025).

Acknowledgements

We thank K. Niedringhaus for validating a subset of the photographs containing coyotes with signs of mange. We also like to thank the many interns and volunteers that helped with fieldwork and processing photos. We also thank the many landowners who allowed us access to their property.

Author contributions

Conceptualization: T.A.G.-C., M.H.M. and M.F. Methodology: T.A.G.-C., MH.M. and M.F. Software: T.A.G.-C., P.R. and M.F. Validation: T.A.G.-C., M.H.M., S.F., B.R.P. and M.F. Formal analysis: T.A.G.-C., M.H.M. and M.F. Investigation: M.H.M., J.A., S.F., D.G., J.D.H., S.H., M.J., J.S.L., R.L., M.M., S.R. and K.R. Resources: P.R., S.F., M.-J.F., P.G., D.G., M.T.K., J.S.L., R.L., L.W., P.K.M., B.R.P., K.R. and C. Shier. Data curation: T.A.G.-C., M.H.M., P.R., J.A., T.G., P.G., J.D.H., L.W., S.H., M.J., J.S.L., R.L., C. Salsbury, C.J. Schell, C.J. Stevenson, J.S.V.S, T.W. and M.M. Writing—original draft: T.A.G.-C., M.H.M. and M.F. Writing—review and editing: T.A.G.-C., M.H.M., S.F., T.G., J.D.H., M.J., M.T.K., J.S.L., S.R., K.R., C. Shier, C. Salsbury, C.J. Schell, C.J. Stevenson, J.S.V.S, T.W. and C.C.S.C. Visualization: T.A.G.-C., M.H.M. and M.F. Supervision: M.H.M., S.M. and M.F. Project administration: T.A.G.-C., M.H.M., T.G., M.J., J.S.L., K.R., T.R., C. Shier, C.C.S.C. and M.F. Funding acquisition: M.H.M., M.-J.F., T.G., M.T.K., J.S.L., R.L., S.R., C. Shier, S.M. and M.F.

Funding
This paper is based on work supported by the National Science Foundation under grant no. 2307324. The funding agencies had no role in the study design, data collection and analysis, decision to publish or preparation of the paper.

Competing interests
The authors declare no competing interests.

Additional information
Extended data is available for this paper at https://doi.org/10.1038/s44284-026-00501-4.

Supplementary information The online version contains supplementary material available at https://doi.org/10.1038/s44284-026-00501-4.

Correspondence and requests for materials should be addressed to Tiziana A. Gelmi-Candusso or Maureen H. Murray.

Peer review information *Nature Cities* thanks Daniel Becker, Kimberly Hall and Pablo Palencia for their contribution to the peer review of this work.

[1]Lincoln Park Zoo, Chicago, IL, USA. [2]University of Toronto, Toronto, Ontario, Canada. [3]Butler University, Indianapolis, IN, USA. [4]University of Georgia, Athens, GA, USA. [5]University of Maryland, Washington DC, MD, USA. [6]Indiana University, Indianapolis, IN, USA. [7]Arizona State University, Mesa, AZ, USA. [8]University of Washington, Seattle, WA, USA. [9]Seattle University, Seattle, WA, USA. [10]Woodland Park Zoo, Seattle, WA, USA. [11]University of Toronto Scarborough, Toronto, Ontario, Canada. [12]Ontario Ministry of Natural Resources, Peterborough, Ontario, Canada. [13]University of Alberta, Edmonton, Alberta, Canada. [14]University of California, Berkeley, Berkeley, CA, USA. [15]City of Edmonton, Edmonton, Alberta, Canada. [16]San Francisco Recreation and Park Department, San Francisco, CA, USA. ✉e-mail: tgelmicandusso@lpzoo.org; maureenmurray@lpzoo.org

https://doi.org/10.1038/s44284-026-00501-4

Extended Data Table 1 | Distribution of coyote presence and mange occurrence across sites. Sampling summary across cities, including seasonal range of sampling, for each city, total number of seasons, weeks, and sites sampled, number of sites whereby at least one coyote was detected (sites with coyotes), and whereby at least one coyote with mange was detected (sites with mange), and naive occupancy for coyotes and for mange, that is, proportion of sites sampled where coyotes or mange were present at least once

City	Temporal range	Sampling seasons	Sampling weeks	Sampling sites	Sites w/ coyotes	Sites w/ mange	Coyote naïve occupancy	Mange naïve occupancy
Phoenix, AZ	SP19 – WI20	4	1371	47	40	30	0.85	0.75
Toronto, ON	FA20 – SU21	4	736	25	21	15	0.84	0.71
East Bay, CA	SP22 – FA22	3	367	36	13	7	0.36	0.54
Seattle, WA	WI20 – WI21	4	1320	37	22	11	0.59	0.50
Chicago, IL	WI19 – FA19	4	3209	112	76	37	0.67	0.49
Indianapolis, IN	FA18 – WI20	6	539	42	41	18	0.98	0.44
San Francisco, CA	FA19 – WI21	6	1576	31	29	7	0.94	0.24
Washington, DC	SU20 – FA22	10	4568	77	39	6	0.51	0.15
Edmonton, AL	WI19 – FA19	4	732	29	29	4	1.00	0.14
Atlanta, GA	SP22 – WI23	4	1622	51	46	4	0.90	0.09

https://doi.org/10.1038/s44284-026-00501-4

Extended Data Table 2 | Coyote and mange occupancy across cities and the city-specific average effect size of urbanization and landscape connectivity. City-specific average occupancy of coyote and mange conditional of coyote presence. For the effect of urbanization and landscape connectivity on predicted occupancy we included the probability of a city following the overall results based on the proportion of iterations resulting in an estimated effect size above zero (positive effect) or below zero (negative effect). These overall results were negative for urbanization on coyote (−) and positive for urbanization on mange (+) and for local landscape connectivity on coyote (+) and mange (+). For each city, the median effect size of urbanization and landscape connectivity and its 90% credible intervals are provided within []. All estimates include 90% confidence intervals in parentheses

City	Average Occupancy		Urbanization		Landscape Connectivity	
	Coyote	Mange | Coyote	Coyote	Mange | Coyote	Coyote	Mange | Coyote
Atlanta, GA	0.51 (0.05, 0.95)	0.52 (0.05, 0.92)	0.96 [B = −0.40 (−0.80, −0.03)]	0.70 [B = 0.32 (−0.70, 1.42)]	0.89 [B = 0.24 (−0.09, 0.57)]	0.74 [B = 0.38 (−0.62, 1.48)]
East Bay Area, CA	0.48 (0.04, 0.96)	0.66 (0.12, 0.98)	1.00 [B = −0.62 (−1.04, −0.27)]	0.66 [B = 0.31 (−1.03, 1.58)]	0.00 [B = −0.84 (−1.45, −0.31)]	0.77 [B = 0.62 (−0.88, 2.22)]
Chicago, IL	0.59 (0.16, 0.93)	0.71 (0.23, 0.97)	1.00 [B = −0.35 (−0.55, −0.19)]	0.91 [B = 0.57 (−0.14, 1.38)]	0.69 [B = 0.06 (−0.15, 0.28)]	0.97 [B = 0.90 (0.14, 1.75)]
Edmonton, AL	0.38 (0.02, 0.96)	0.53 (0.04, 0.94)	0.46 [B = 0.02 (−0.35, 0.42)]	0.89 [B = 0.59 (−0.20, 1.54)]	0.99 [B = 0.43 (0.12, 0.79)]	0.83 [B = 0.48 (−0.32, 1.50)]
Indianapolis, IN	0.90 (0.33, 1.00)	0.73 (0.22, 0.98)	0.70 [B = −0.28 (−1.17, 0.64)]	0.93 [B = 0.69 (−0.07, 1.60)]	0.45 [B = −0.08 (−1.31, 1.00)]	0.73 [B = 0.24 (−0.44, 0.91)]
Washington DC	0.22 (0.03, 0.71)	0.66 (0.19, 0.96)	0.98 [B = −0.33 (−0.66, −0.06)]	0.59 [B = 0.16 (−1.07, 1.35)]	0.72 [B = 0.16 (−0.37, 0.59)]	0.75 [B = 0.50 (−0.76, 1.85)]
Phoenix, AZ	0.62 (0.06, 0.99)	0.67 (0.12, 0.97)	0.95 [B = −0.64 (−1.27, −0.01)]	0.01 [B = −0.37 (−0.67, −0.10)]	0.35 [B = −0.20 (−1.21, 0.65)]	0.48 [B = −0.01 (−(−0.43, 0.40)]
San Francisco, CA	0.80 (0.22, 0.99)	0.58 (0.08, 0.95)	0.97 [B = −0.25 (−0.49, −0.03)]	0.73 [B = 0.30 (−0.59, 1.15)]	0.48 [B = −0.01 (−0.49, 0.45)]	0.90 [B = 0.98 (−0.29, 2.55)]
Seattle, WA	0.12 (0.01, 0.70)	0.51 (0.05, 0.92)	0.52 [B = −0.01 (−0.21, 0.20)]	0.01 [B = −0.53 (−0.95, −0.18)]	0.17 [B = −0.17 (−0.47, 0.12)]	0.56 [B = 0.05 (−0.50, 0.64)]
Toronto, ON	0.79 (0.31, 0.98)	0.81 (0.35, 0.99)	0.86 [B = −0.33 (−0.84, 0.17)]	0.89 [B = 0.73 (−0.25, 1.83)]	1.00 [B = 1.49 (0.72, 2.56)]	0.98 [B = 1.24 (0.24, 2.51)]

https://doi.org/10.1038/s44284-026-00501-4

Extended Data Table 3 | The effect of city-specific environmental covariates on coyote occupancy and mange occurrence conditional of coyote occupancy. Bold text reflects covariates with >90% likelihood of having an effect with the defined directionality on coyote occupancy (left) and mange occurrence (right)

Among-city Covariate	Coyote occupancy			Mange occurrence		
	Likelihood	Directionality	Effect size	Likelihood	Directionality	Effect size
Urban population density	**81%**	**negative**	**(−0.69 90% BCI, −2.02 to 0.66)**	**91%**	**positive**	**(+1.19 90% BCI, −0.28 to 2.69)**
Natural surface cover	**81%**	**positive**	**(+0.65 90% BCI, −0.58 to 2.06)**	57%	positive	(+0.13 90% BCI, −1.09 to 1.29)
Urban vegetation density	57%	negative	(−0.10 90% BCI, −1.24 to 0.99)	**95%**	**negative**	**(−1.23 90% BCI, −2.38 to −0.01)**
Movement Corridor abundance	55%	positive	(+0.06 90% BCI, −0.87 to 0.90)	**97%**	**negative**	**(−1.34 90% BCI, −2.59 to −0.17)**
Winter harshness	55%	positive	(+0.05 90% BCI, −0.75 to 0.85)	**89%**	**negative**	**(−0.59 90% BCI, −1.41 to 0.22)**
Relative Humidity	56%	positive	(+0.09 90% BCI, −0.97 to 1.21)	**75%**	**positive**	**(+0.36 90% BCI, −0.55 to 1.31)**

https://doi.org/10.1038/s44284-026-00501-4

Extended Data Table 4 | Projected change rates for human population, chilling days (that is, winter severity), and relative humidity across the most sustainable and least sustainable future socioeconomic pathways (SSPs) and forecasted change in mange average occupancy across cities following those forecasted environmental changes

City		SSP126			SSP585		
	Population growth rate	Chilling-days	Relative humidity	Mange occurrence change	Chilling-days	Relative humidity	Mange occurrence change
Edmonton	1.501	0.86	1.02	+0.30	0.79	1.04	+0.33
Toronto	1.182	0.84	0.99	+0.18	0.71	0.99	+0.20
Washington DC	1.153	0.74	0.95	+0.15	0.63	0.96	+0.16
Phoenix	1.284	0.79	0.96	+0.13	0.72	0.96	+0.13
Indianapolis	1.155	0.7	0.96	+0.11	0.61	0.97	+0.12
Chicago	1.146	0.68	0.97	+0.09	0.59	0.98	+0.12
Seattle	1.217	0.63	0.97	+0.08	0.56	0.98	+0.10
Atlanta	1.268	0.91	0.97	+0.10	0.81	0.97	+0.09
East Bay	1.179	0.83	0.98	+0.01	0.76	0.98	+0.01
San Francisco	0.909	0.78	0.99	−0.02	0.72	0.99	−0.02

https://doi.org/10.1038/s44284-026-00501-4

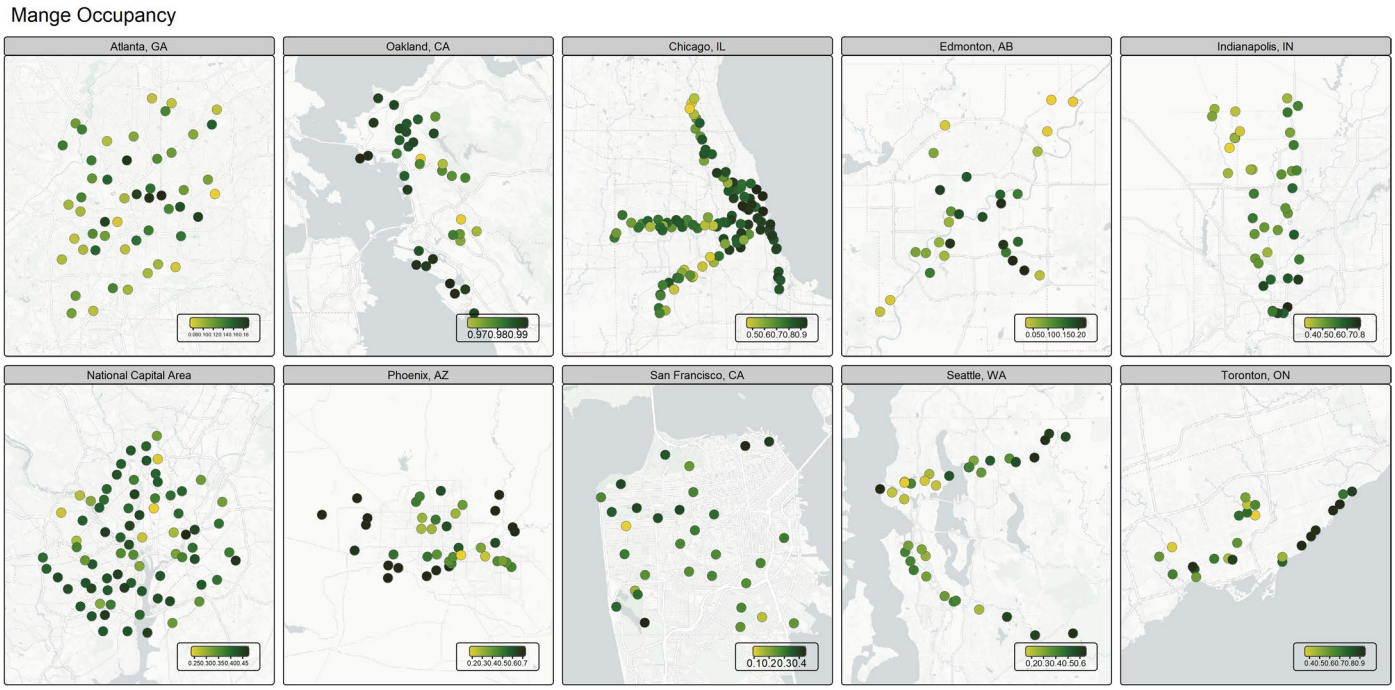

Extended Data Fig. 1 | Mange occurrence along the urban–rural gradient and across diverse urban landscape configurations. Site-level predictions of mange occurrence across cities considering local environmental conditions in terms of urbanization and landscape connectivity. Map tiles from CartoDB © and OpenStreetMap contributors.

https://doi.org/10.1038/s44284-026-00501-4

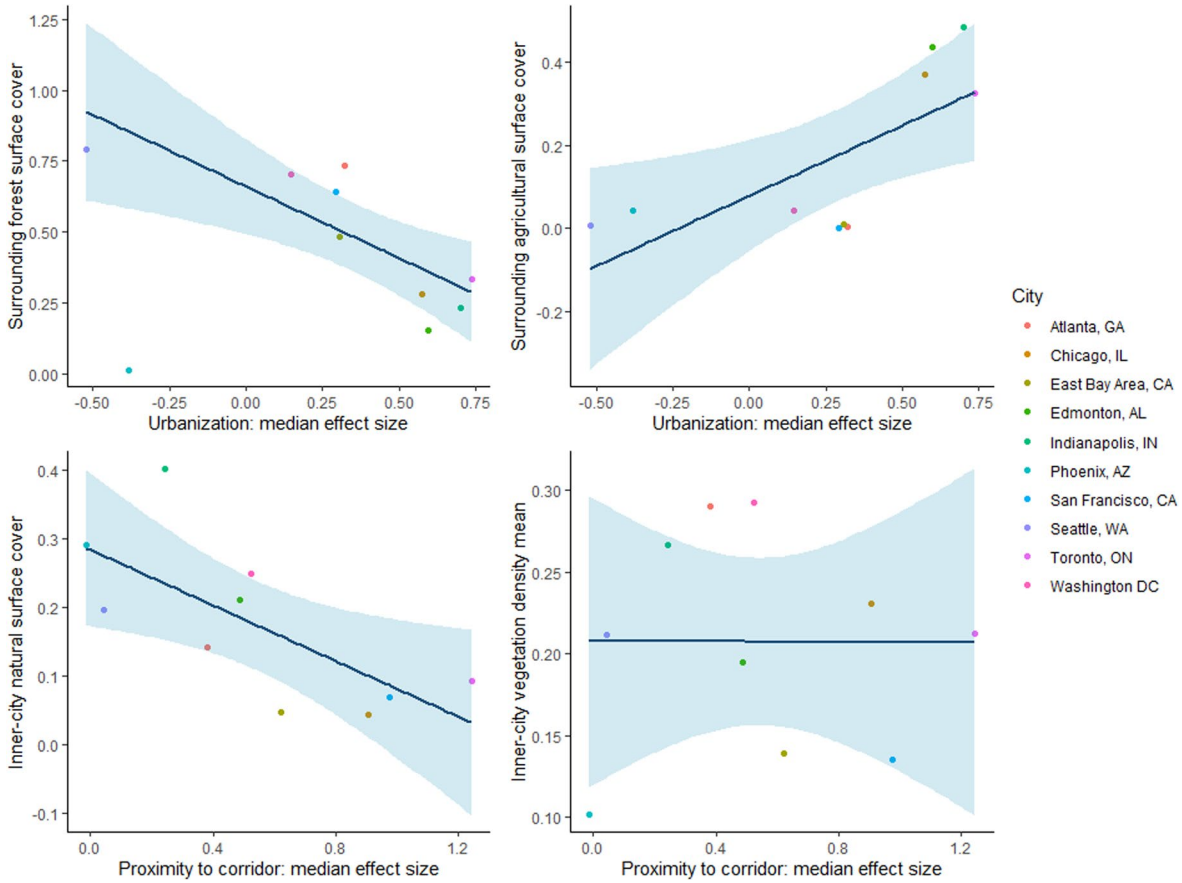

Extended Data Fig. 2 | City-level landscape context modulates the effects of urbanization and connectivity at the site-level. Relationship between median effect size, across cities, of urbanization and surrounding landscape cover (top) and of proximity to corridor and inner landscape cover (bottom), ribbons show confidence intervals of linear regression (line) of effect sizes observed across cities and the surrounding or inner-city characteristics (n=10). Note: Phoenix was not included in the forest cover regression estimate (line, top left) as its surrounding natural habitat type is not characterized by forest cover.

https://doi.org/10.1038/s44284-026-00501-4

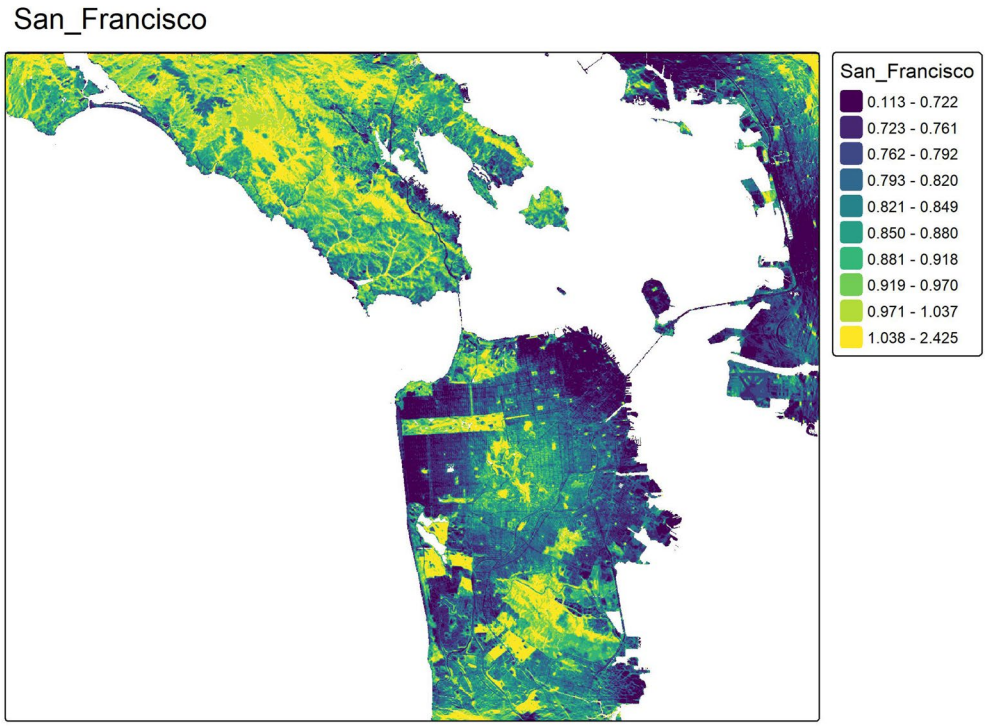

Extended Data Fig. 3 | Landscape connectivity of a coastal city. Example of connectivity output for a city surrounded by water, San Francisco, shown as normalized current density categorized in 10 percentiles.

https://doi.org/10.1038/s44284-026-00501-4

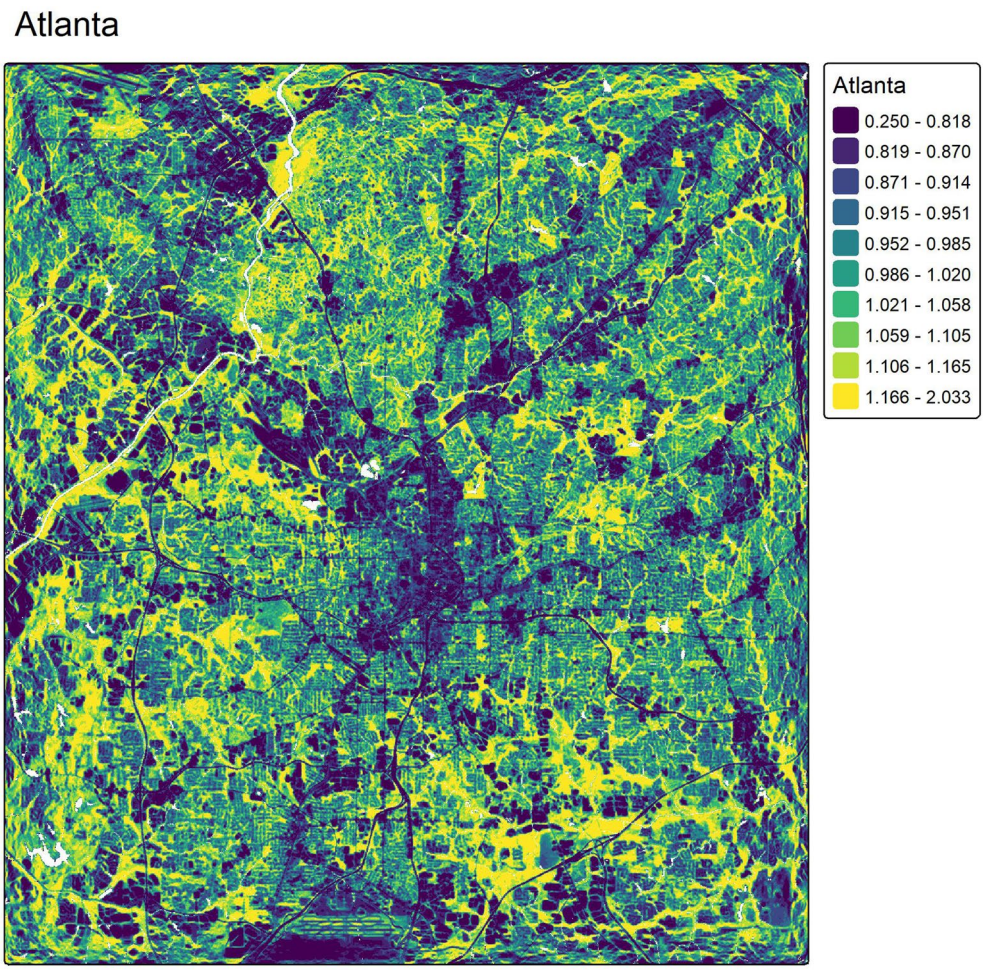

Extended Data Fig. 4 | Landscape connectivity of an inland city. Example of connectivity output for a city surrounded by land, Atlanta, shown as normalized current density categorized in 10 percentiles.

nature portfolio

Corresponding author(s): Gelmi-Candusso T.A. and Murray M.H.

Last updated by author(s): Jun 25, 2026

Reporting Summary

Nature Portfolio wishes to improve the reproducibility of the work that we publish. This form provides structure for consistency and transparency in reporting. For further information on Nature Portfolio policies, see our Editorial Policies and the Editorial Policy Checklist.

Statistics

For all statistical analyses, confirm that the following items are present in the figure legend, table legend, main text, or Methods section.

n/a	Confirmed	
☐	☒	The exact sample size (*n*) for each experimental group/condition, given as a discrete number and unit of measurement
☐	☒	A statement on whether measurements were taken from distinct samples or whether the same sample was measured repeatedly
☐	☒	The statistical test(s) used AND whether they are one- or two-sided *Only common tests should be described solely by name; describe more complex techniques in the Methods section.*
☐	☒	A description of all covariates tested
☒	☐	A description of any assumptions or corrections, such as tests of normality and adjustment for multiple comparisons
☐	☒	A full description of the statistical parameters including central tendency (e.g. means) or other basic estimates (e.g. regression coefficient) AND variation (e.g. standard deviation) or associated estimates of uncertainty (e.g. confidence intervals)
☒	☐	For null hypothesis testing, the test statistic (e.g. *F*, *t*, *r*) with confidence intervals, effect sizes, degrees of freedom and *P* value noted *Give P values as exact values whenever suitable.*
☐	☒	For Bayesian analysis, information on the choice of priors and Markov chain Monte Carlo settings
☐	☒	For hierarchical and complex designs, identification of the appropriate level for tests and full reporting of outcomes
☐	☒	Estimates of effect sizes (e.g. Cohen's *d*, Pearson's *r*), indicating how they were calculated

Our web collection on statistics for biologists contains articles on many of the points above.

Software and code

Policy information about availability of computer code

Data collection	no software was used to collect data
Data analysis	Code is available on Github at https://github.com/tgelmi-candusso/CTwildlifedisease (Zenodo archive: 10.5281/zenodo.17210906)

For manuscripts utilizing custom algorithms or software that are central to the research but not yet described in published literature, software must be made available to editors and reviewers. We strongly encourage code deposition in a community repository (e.g. GitHub). See the Nature Portfolio guidelines for submitting code & software for further information.

Data

Policy information about availability of data

All manuscripts must include a data availability statement. This statement should provide the following information, where applicable:

- Accession codes, unique identifiers, or web links for publicly available datasets
- A description of any restrictions on data availability
- For clinical datasets or third party data, please ensure that the statement adheres to our policy

Data is available on Github at https://github.com/tgelmi-candusso/CTwildlifedisease (Zenodo archive: 10.5281/zenodo.17210906)

Research involving human participants, their data, or biological material

Policy information about studies with human participants or human data. See also policy information about sex, gender (identity/presentation), and sexual orientation and race, ethnicity and racism.

Reporting on sex and gender	*Use the terms sex (biological attribute) and gender (shaped by social and cultural circumstances) carefully in order to avoid confusing both terms. Indicate if findings apply to only one sex or gender; describe whether sex and gender were considered in study design; whether sex and/or gender was determined based on self-reporting or assigned and methods used. Provide in the source data disaggregated sex and gender data, where this information has been collected, and if consent has been obtained for sharing of individual-level data; provide overall numbers in this Reporting Summary. Please state if this information has not been collected. Report sex- and gender-based analyses where performed, justify reasons for lack of sex- and gender-based analysis.*
Reporting on race, ethnicity, or other socially relevant groupings	*Please specify the socially constructed or socially relevant categorization variable(s) used in your manuscript and explain why they were used. Please note that such variables should not be used as proxies for other socially constructed/relevant variables (for example, race or ethnicity should not be used as a proxy for socioeconomic status). Provide clear definitions of the relevant terms used, how they were provided (by the participants/respondents, the researchers, or third parties), and the method(s) used to classify people into the different categories (e.g. self-report, census or administrative data, social media data, etc.) Please provide details about how you controlled for confounding variables in your analyses.*
Population characteristics	*Describe the covariate-relevant population characteristics of the human research participants (e.g. age, genotypic information, past and current diagnosis and treatment categories). If you filled out the behavioural & social sciences study design questions and have nothing to add here, write "See above."*
Recruitment	*Describe how participants were recruited. Outline any potential self-selection bias or other biases that may be present and how these are likely to impact results.*
Ethics oversight	*Identify the organization(s) that approved the study protocol.*

Note that full information on the approval of the study protocol must also be provided in the manuscript.

Field-specific reporting

Please select the one below that is the best fit for your research. If you are not sure, read the appropriate sections before making your selection.

☐ Life sciences ☐ Behavioural & social sciences ☒ Ecological, evolutionary & environmental sciences

For a reference copy of the document with all sections, see nature.com/documents/nr-reporting-summary-flat.pdf

Ecological, evolutionary & environmental sciences study design

All studies must disclose on these points even when the disclosure is negative.

Study description	Observational cross-sectional study examining sarcoptic mange (Sarcoptes scabiei) occurrence in urban coyotes (Canis latrans) across 10 North American cities using camera traps. Predictors include urbanization intensity, habitat connectivity, and climate variables. Response variable is coyote occupancy and mange occurrence. No experimental manipulation was performed.
Research sample	Free-ranging urban coyotes (Canis latrans) detected via camera trap networks across 10 North American cities. Animals were not captured or manipulated; detections are opportunistic via passive monitoring. The sample is meant to represent urban coyote populations across a range of North American socio-environmental contexts. Data derived from an existing multi-city camera trap dataset (UWIN).
Sampling strategy	Camera trap networks deployed across urban gradients within each city. Sample size (minimum of 20 sites per city) was determined by existing network sampling design. Unit of analysis for occupancy modeling was site-level detection histories .
Data collection	Passive camera trap monitoring at fixed sites across urban land-use gradients. Mange presence/absence was assessed from photographs by trained observers. Landscape covariates (urbanization, connectivity) were derived from remotely sensed spatial data.
Timing and spatial scale	Spatial scale spans 10 North American cities at the continental scale, with within-city site-level resolution. Temporal scale spans between 2019 and 2022.
Data exclusions	Ambiguous mange classifications were excluded
Reproducibility	Mange presence absence data, occupancy model code and covariate data are available to allow reproduction of results
Randomization	Study sites were randomly allocated within the sampling design
Blinding	Site locations were unknown to the subjects tagging the mange symptoms in the coyote images.

Did the study involve field work? ☒ Yes ☐ No

Field work, collection and transport

Field conditions	Field conditions varied across the year as the sampling seasons included all four seasons throughout multiple years.
Location	Ten cities in North America, only images collected, specific locations obscured for wildlife welfare
Access & import/export	Permits and data agreements were signed with the specific municipalities to set up camera traps and protect sensitive information.
Disturbance	No disturbance caused on sites

Reporting for specific materials, systems and methods

We require information from authors about some types of materials, experimental systems and methods used in many studies. Here, indicate whether each material, system or method listed is relevant to your study. If you are not sure if a list item applies to your research, read the appropriate section before selecting a response.

Materials & experimental systems

n/a	Involved in the study
☒	☐ Antibodies
☒	☐ Eukaryotic cell lines
☒	☐ Palaeontology and archaeology
☐	☒ Animals and other organisms
☒	☐ Clinical data
☒	☐ Dual use research of concern
☒	☐ Plants

Methods

n/a	Involved in the study
☒	☐ ChIP-seq
☒	☐ Flow cytometry
☒	☐ MRI-based neuroimaging

Animals and other research organisms

Policy information about studies involving animals; ARRIVE guidelines recommended for reporting animal research, and Sex and Gender in Research

Laboratory animals	the study did not involve laboratory animals
Wild animals	Images of coyotes (Canis latrans) were collected using camera traps.
Reporting on sex	sex is not identifiable from camera trap images
Field-collected samples	the study did not involve collection of samples from the field
Ethics oversight	Ethical oversight was present for the treatment of human images captured on camera trap data, these were disposed off before species classification of wild animals.

Note that full information on the approval of the study protocol must also be provided in the manuscript.

Plants

Seed stocks	*Report on the source of all seed stocks or other plant material used. If applicable, state the seed stock centre and catalogue number. If plant specimens were collected from the field, describe the collection location, date and sampling procedures.*
Novel plant genotypes	*Describe the methods by which all novel plant genotypes were produced. This includes those generated by transgenic approaches, gene editing, chemical/radiation-based mutagenesis and hybridization. For transgenic lines, describe the transformation method, the number of independent lines analyzed and the generation upon which experiments were performed. For gene-edited lines, describe the editor used, the endogenous sequence targeted for editing, the targeting guide RNA sequence (if applicable) and how the editor was applied.*
Authentication	*Describe any authentication procedures for each seed stock used or novel genotype generated. Describe any experiments used to assess the effect of a mutation and, where applicable, how potential secondary effects (e.g. second site T-DNA insertions, mosiacism, off-target gene editing) were examined.*